Distribution Category:
Environmental Control Technology
and Earth Sciences (UC-11)

ANL-82-65
Part IV

ANL--82-65-Pt.4

DE84 009129

ARGONNE NATIONAL LABORATORY
9700 South Cass Avenue
Argonne, Illinois 60439

RADIOLOGICAL AND ENVIRONMENTAL RESEARCH DIVISION ANNUAL REPORT

Atmospheric Physics
January—December 1982

A. F. Stehney, Acting Director
M. L. Wesely, Section Head

January 1984

Preceding Report

ANL-81-85 Part IV January—December 1981

FOREWORD

The Atmospheric Physics Section investigates the physical behavior of the lower atmosphere and some of its chemical properties. Scientific research is conducted primarily in response to specific needs of sponsors and usually addresses some overall goal identified by funding agencies. For example, research pertinent to the "acid rain" issue comprised the bulk of our work in 1982. In this report we emphasize work for the U. S. Department of Energy (DOE) and closely related projects. Since in calendar year 1982 the EPA supported most of our research related to acid deposition, much of that work has been reported elsewhere and is not fully represented here. For all phases of research by this Section, more thorough accounts can be found in the open scientific literature.

Work on mean and turbulent flow characteristics in the planetary boundary layer (PBL) over nonuniform terrain continues to be the major emphasis of our research for DOE, specifically for the Atmospheric Studies over Complex Terrain (ASCOT) program of DOE/OHER. The first article in this report, although dealing with simple terrain, summarizes an effort to obtain measures of parameters important in transport and diffusion in the lower atmosphere solely by use of a Doppler acoustic sounding system. These techniques might apply to a limited extent to flow over complex terrain, where acquisition of such data by traditional techniques might be exceedingly difficult. Analyses carried out in 1982 of data collected by ANL during the large ASCOT experiment in 1980 on flow over the mountainous region of the California Geysers area are not described in this report, but the results have been summarized in a topical report entitled "Remote Sensing of Winds and Turbulence above Complex Terrain During ASCOT-1980" (ANL/ER-83-1). The second article describes participation in a multiagency experiment (Shoreline Environment Atmospheric Dispersion Experiment, SEADEX) to study the fate of materials released over a surface with notable surface nonuniformities, specifically at a coastal nuclear power plant during onshore flow conditions.

The second and third articles in this report address research on the local behavior of pollutants emitted from diesel engines in urban areas. This work was done as part of a DOE project in which participation by this Secton ended in FY 1982. In 1982, as in 1981, most effort was directed toward field

studies on circulation patterns in street canyons, exchange rates with the atmosphere above rooftops, and characterization of particles in outdoor urban microclimates. This work is described in a Ph.D. thesis by Dr. F. T. DePaul.

The remainder of this report is quite diverse and contains multiple articles on perhaps only one or two types of research. One is numerical modeling of the behavior of atmospheric pollutants, especially gaseous and particulate substances associated with acid deposition. The modeling and theoretical capabilities have been developed in part to consider potential nonlinear relationships between anthropogenic emissions of sulfur and nitrogen compounds and the distant deposition of resulting acidifying substances. On the experimental side, field phases of research designed to compare methods of analyses of precipitation samples and to study local urban effects on precipitation chemistry were completed in FY 1982.

TABLE OF CONTENTS

THE VOICE EXPERIMENT--PRELIMINARY RESULTS

R. L. Coulter, T. J. Martin, and K. H. Underwood

The Vertical Observations Including Convective Exchange (VOICE) experiment was conducted from 18 June 1982 to 30 June 1982 by the Atmospheric Physics Section in conjunction with the Dry Deposition Intercomparison Experiment (DDIE). The purpose of the VOICE experiment was to make detailed observations of the convective vertical velocity field of the planetary boundary layer (PBL) with the Doppler sodar as part of a preliminary effort to measure vertical velocities within and near fair-weather clouds. The DDIE provided measurements of such crucial surface-layer-boundary conditions as heat, momentum and water vapor fluxes, radiation balances, and surface-layer winds and temperatures. Additional activities for VOICE included monitoring of clouds through use of a time-lapse camera and making simultaneous double-theodolite observations to determine the mixing condensation level, cloud height, and cloud position during times propitious for the measurement of near-cloud velocities.

A related part of this investigation was use of the sodar to estimate surface heat flux in order to provide area-averaged estimates that are more representative of nonhomogeneous conditions, e. g., regions with multiple crops. The sodar was located near the northern edge of a large grass field (Figure 1); to the north was a field of soybeans and to the northeast was a field of corn. Previous investigations (Coulter and Wesely, 1980) demonstrated the feasibility of analyzing sodar signal amplitudes to obtain estimates of surface heat flux under a variety of conditions. With the additional Doppler capability, however, it might be possible to estimate the heat flux profile within the well-mixed layer under unstable conditions through measurements of the standard deviation of vertical velocity, σ_w.

Several researchers (e.g., Panofsky and McCormick, 1960; Caughey and Readings, 1974) have observed that in the surface layer and lower part of the PBL, σ_w can be expressed as:

$$\sigma_w/u_* \sim (z/L)^{1/3}, \qquad (1)$$

where u_* is the surface friction velocity and L is the Monin-Obukhov length. This formulation ensures that σ_w is not a function of u_*, i. e., convective conditions prevail. From the functional relationship for L, the heat flux H can be expressed as:

$$H = B(\sigma_w^3/z) \quad , \tag{2}$$

where B is constant. Weill et al. (1980) used this approach with sodar data to successfully evaluate heat flux during the morning. It should be noted, however, that σ_w becomes nearly constant with height in the upper convective boundary layer. Thus, it is necessary to exercise care in selecting the height interval so as to avoid the nonlinear region located above the region where Eq. (2) is valid.

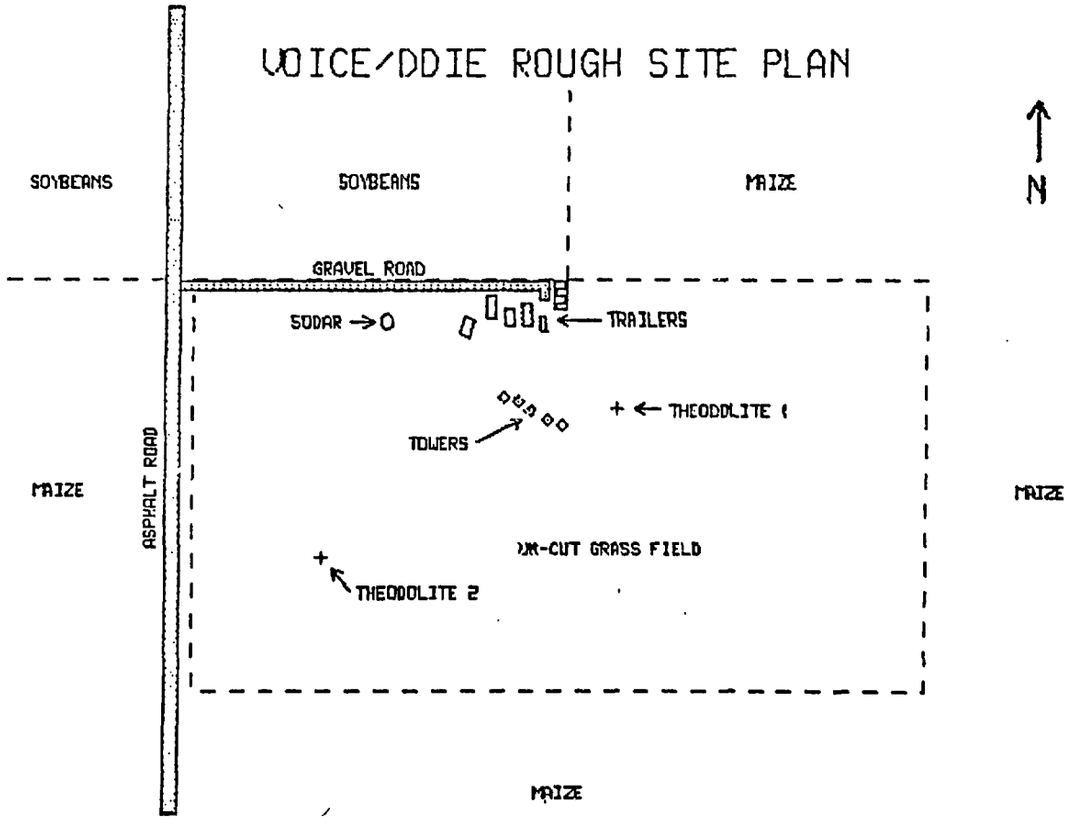

Fig. 1. Plan view of the position of instruments and nearby crops.

A typical profile of σ_w^3/z from the VOICE experiment is illustrated in Figure 2. Nonlinearity of the profile very near the surface is possible if mechanically generated turbulence is sufficient to increase substantially the value of σ_w. Values derived at high altitudes must be examined with care because there is often a reduced statistical sample size resulting from selective signal processing of only the larger signal levels. Extension of the linear portion of the profile to zero provides an estimate of the height of zero vertical heat flux, which is estimated to be approximately 70% of the height of the well-mixed layer (Deardorff, 1974).

Estimates of heat fluxes and heights of zero heat flux from these methods, as well as mixed-layer heights derived from the sodar amplitude records, are shown in Figures 3 and 4. Although the values reported here must be regarded as preliminary, it is apparent that the heat flux estimates do not suffer excessively from the morning overestimates previously noted by Coulter and Wesely (1979). Inversion height estimates in Figure 4 appear to be generally greater than the height of the well-mixed layer. Further experimental investigations are necessary to resolve this discrepancy.

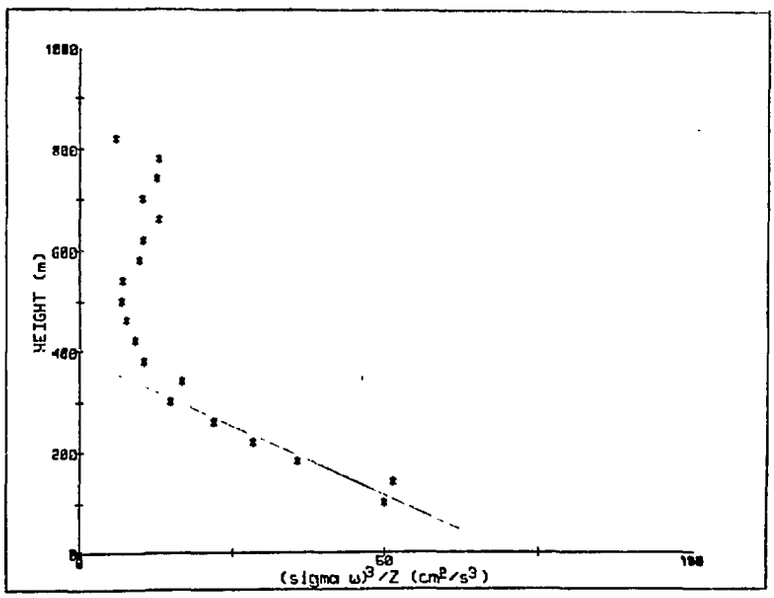

Fig. 2. A typical profile of σ_w^3/z versus height averaged over a one-hour period during the VOICE experiment.

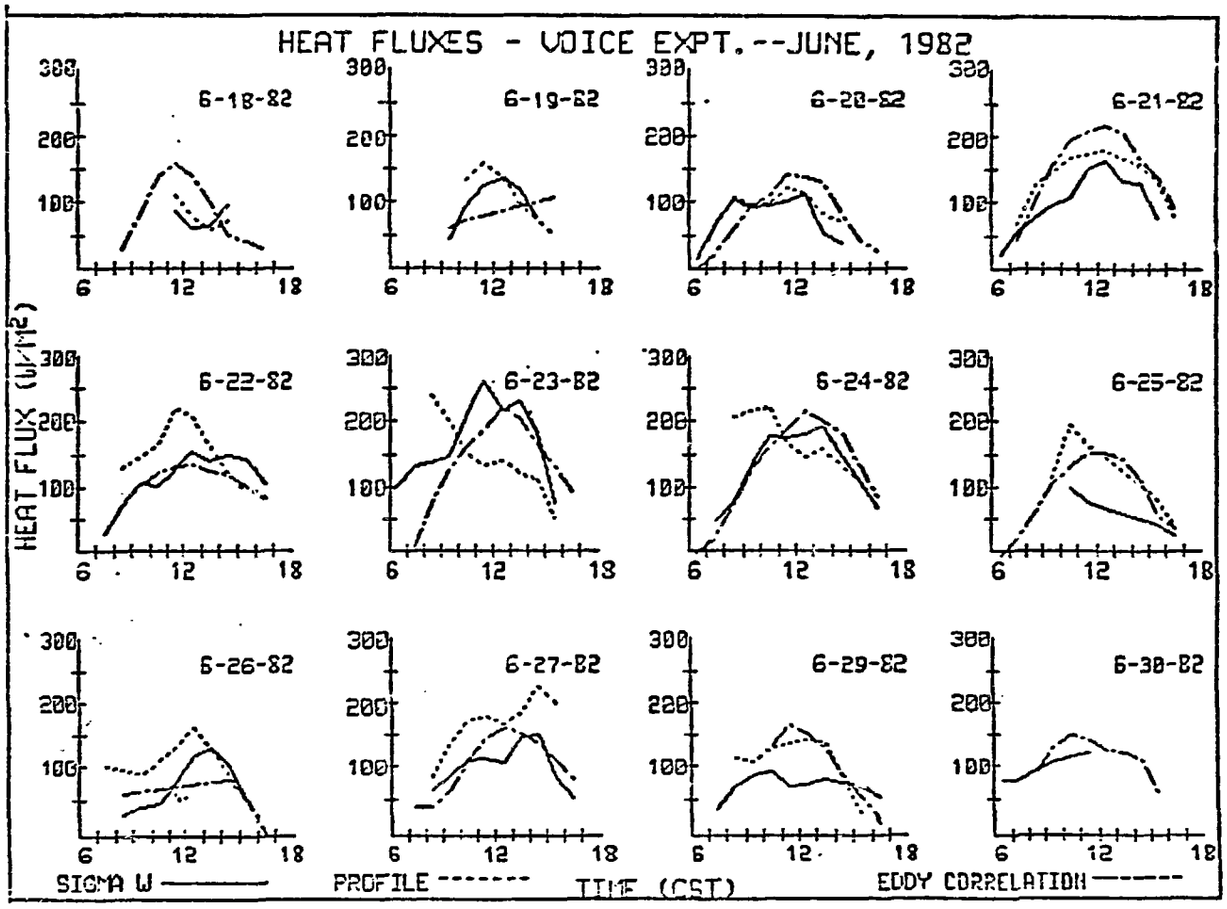

Fig. 3. Hourly values of heat flux derived from σ_w^3/z profiles during the VOICE experiment and from eddy correlation during DDIE.

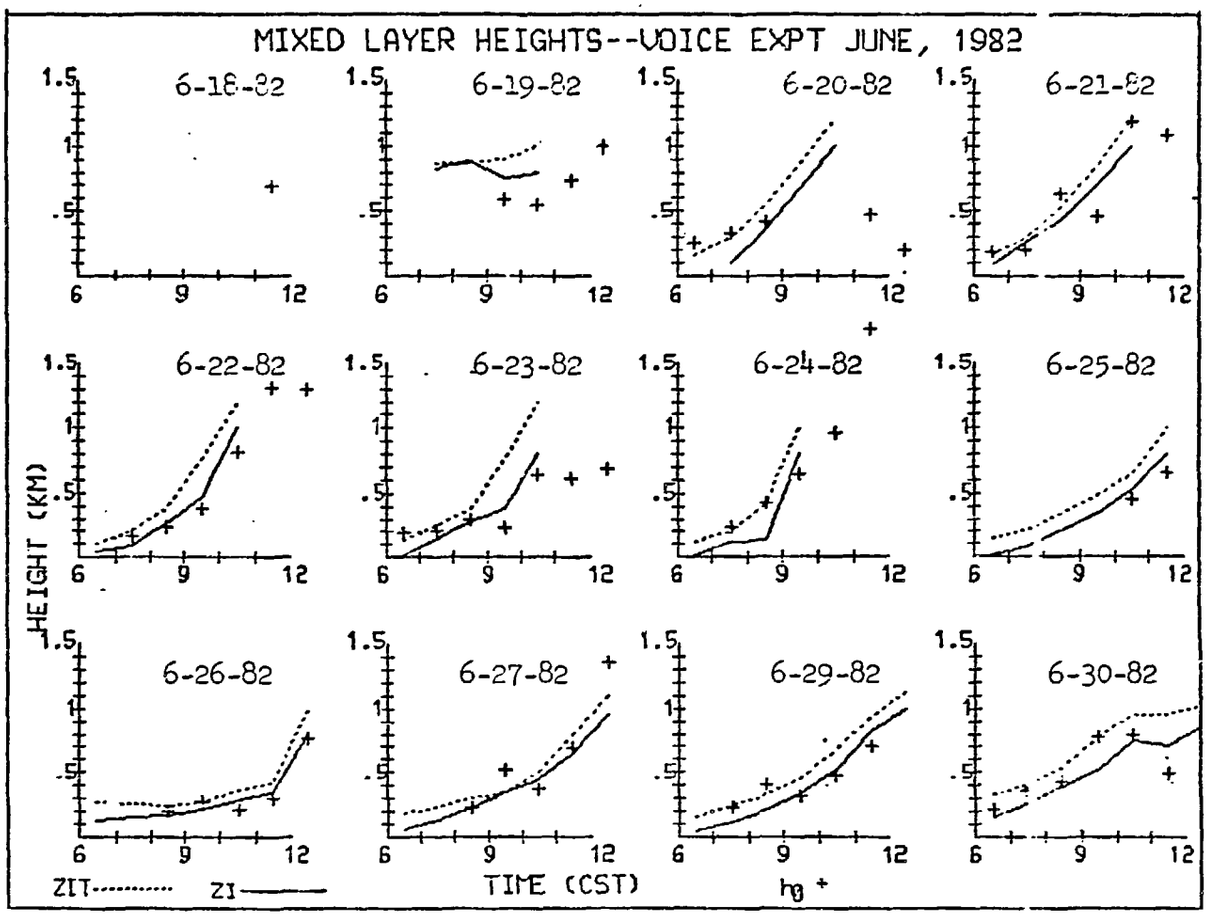

Fig. 4. Hourly estimates the height of zero heat flux (+) and top (——) and bottom (---) of the measured mixed layer height as taken from sodar records during the VOICE experiment.

References

Caughey, S. J. and C. J. Readings, 1974: Vertical component of turbulence in convective conditions, Advances in Geophysics, Vol. 18A, F. N. Frenkiel and R. E. Munn, Eds., Academic Press, New York, pp. 125-130.

Coulter, R. L. and M. L. Wesely, 1980: Estimates of surface heat flux from sodar and laser scintillation measurements in the unstable boundary layer, J. Appl. Meteorol. 10, 1210-1222.

Deardorff, J. N., 1974: Three-dimensional numerical study of the height and mean structure of a heated planetary boundary layer, Boundary-Layer Meteorol. 7, 81-106.

Panofsky, H. A. and R. McCormick, 1960: The spectrum of vertical velocity near the surface, Q. J. R. Meteorol. Soc. 86, 495-503.

Weill, A., C. Klapisz, B. Strauss, F. Baudin and C. Jaupart, 1980: Measuring heat flux and structure functions of temperature fluctuations with an acoustic Doppler sodar, J. Appl. Meteorol. 19, 199-205.

THE SEADEX EXPERIMENT

R. L. Coulter, R. L. Hart, T. J. Martin, K. H. Underwood, and G. A. Zerb

Mesoscale atmospheric circulations created by sharp temperature differ ences at land-water interfaces have been studied by the Atmospheric Physic Section for several years. Large horizontal gradients in temperature, water vapor content, wind speed and direction, and turbulence intensity nea shorelines present a challenge for numerical model prediction. Relative t this problem, the Shoreline Environment Atmospheric Dispersion Experimen (SEADEX), a multilaboratory effort supported principally by the Nuclea Regulatory Commision (NRC), was conducted to study the fate of material released to the atmosphere at coastal nuclear power plants during onshor wind-flow conditions. Principal participants in the study were SR International, the National Oceanic and Atmospheric Administratio Environmental Research Laboratories (NOAA-ERL), and ANL.

The SEADEX study was centered around the Kewaunee, Wisconsin nuclea power plant on the western shore of northern Lake Michigan (Figure 1). Th network included meteorological towers and surface samplers for sulfu hexafluoride (SF_6), which was released 45 m above the surface at the plan site. Tetroons were released hourly from the surface, and an oil fog wa released from the same point as the SF_6. The oil fog was tracked by airborn and mobile surface lidar, while the tetroons, set to remain at selected alti tudes (usually near 150 m), were tracked by NOAA radar.

Argonne operated at two locations: (1) DAWS, a site about 2 miles inlan and 3 miles NNW of the plant and (2) at a site due east of DAWS, about 7 mile offshore. At DAWS, the Doppler sodar was used to continuously monitor th wind and thermal turbulence structure through the lowest 500 m of th atmosphere, and a tethersonde operation was used to obtain wind, temperature and humidity profiles to near 500 m twice an hour. At the offshore sit water temperature was measured and a second tethersonde system provid profiles of wind, temperature, and dewpoint temperature to 500 m.

Throughout the experimental period (20 May 1982 to 10 June 1982), shore flow predominated, with heavy natural fog present during the first f days. Even on days with little fog and strong solar heating, sodar intensi

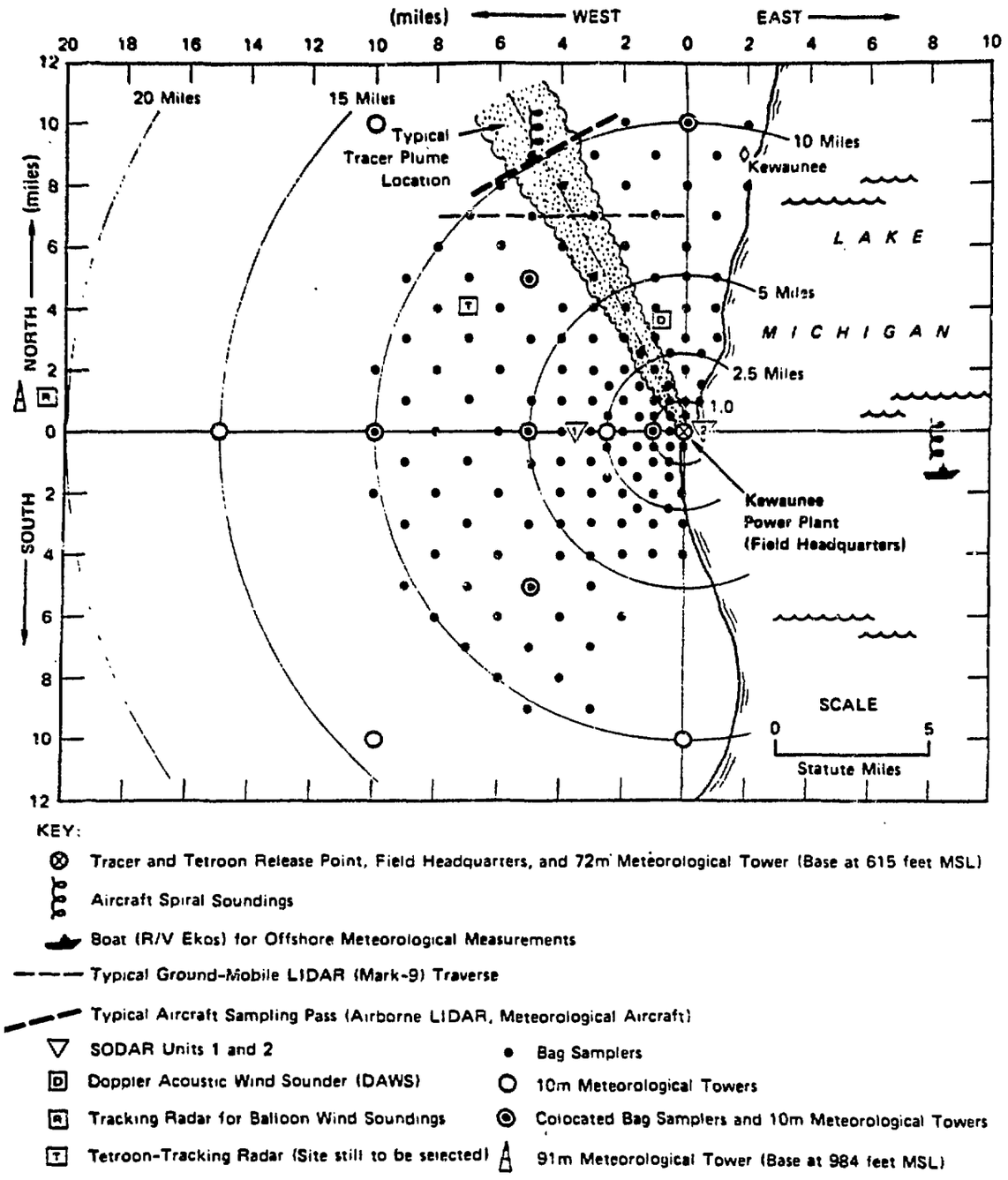

Fig 1. **A depiction of the experimental area and the locations of instruments, samplers, and other devices used in the SEADEX experiment.**

displays indicated that conditions at DAWS rarely became convective. It appears that the air from Lake Michigan was sufficiently stable to prevent the development of significant penetrative convection. Indeed, water temperatures measured at the RV EKOS were quite low, near 4°C throughout the study, with the exception of the final day, when the water temperature was 9°C. This warmer temperature was possibly due to advection of warmer surface water. Air temperature profiles over Lake Michigan indicated very stable atmospheric conditions through the lowest 100 m. Temperature gradients of 10 K/100 m were not uncommon over the water, although the temperature structure was generally modified to gradients of 0 to -0.5 K/100 m through the lowest 100 m (see Fig. 2) by the time the air mass reached DAWS.

A classical lake breeze circulation developed on the final field day of the study, 8 June 1982 (Fig. 3). Onshore flow from NNE-NE veered to easterly after 1000 CST, and a return circulation was evident at both sites after 1100 CST. Surface conditions at the land site remained slightly stable; thus, the lake breeze front was not evident in the sodar intensity record. The return flow continued to develop and was observed as low as 250 m above the sodar site near 1400 CST. An elevated return flow was also seen in the oil fog tracer release, which was tracked returning toward the lake as a well-defined entity displaced to the north.

These data combined with data from the tracers and meteorological towers located within the experimental area should permit detailed analyses of onshore flow regimes and the conditions necessary for development of return flows. Such information is of significant value in developing pollution-dispersion models or evacuation plans.

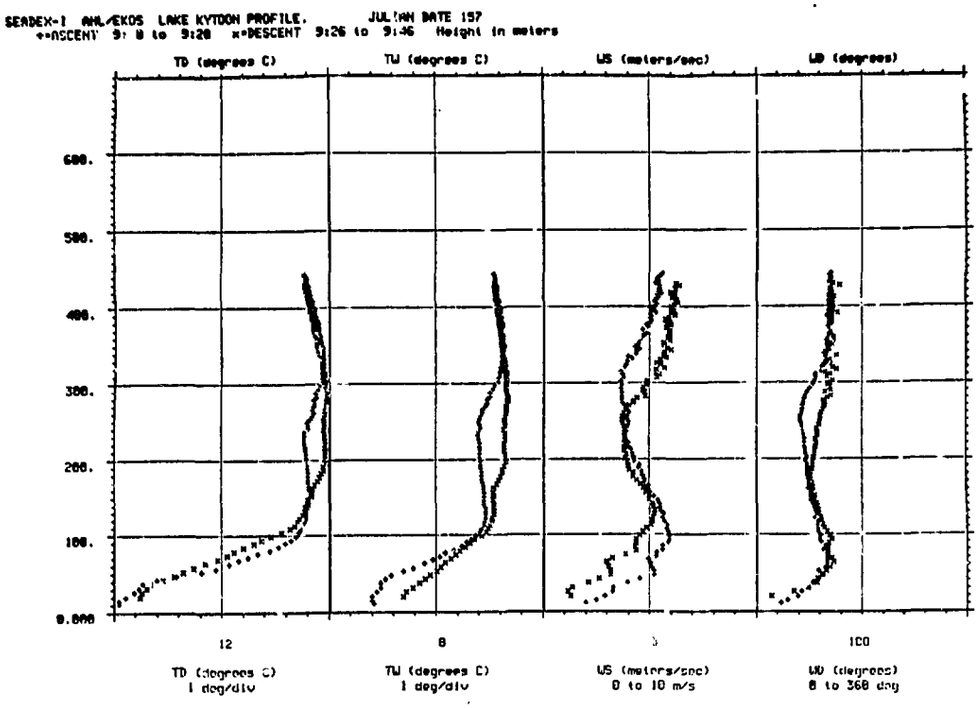

(a)

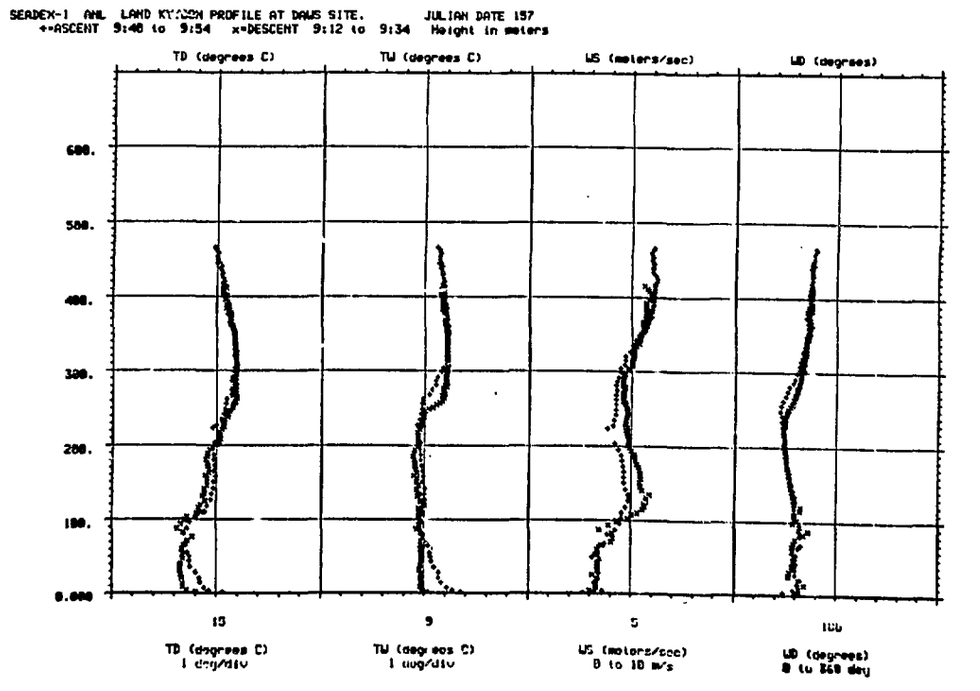

(b)

Fig. 2. Profiles of temperature (TD), dewpoint temperature (TW), wind speed (WS) and wind direction (WD) taken over (a) Lake Michigan from the RV EKOS on June 6, 1982, and (b) the land site two miles inland.

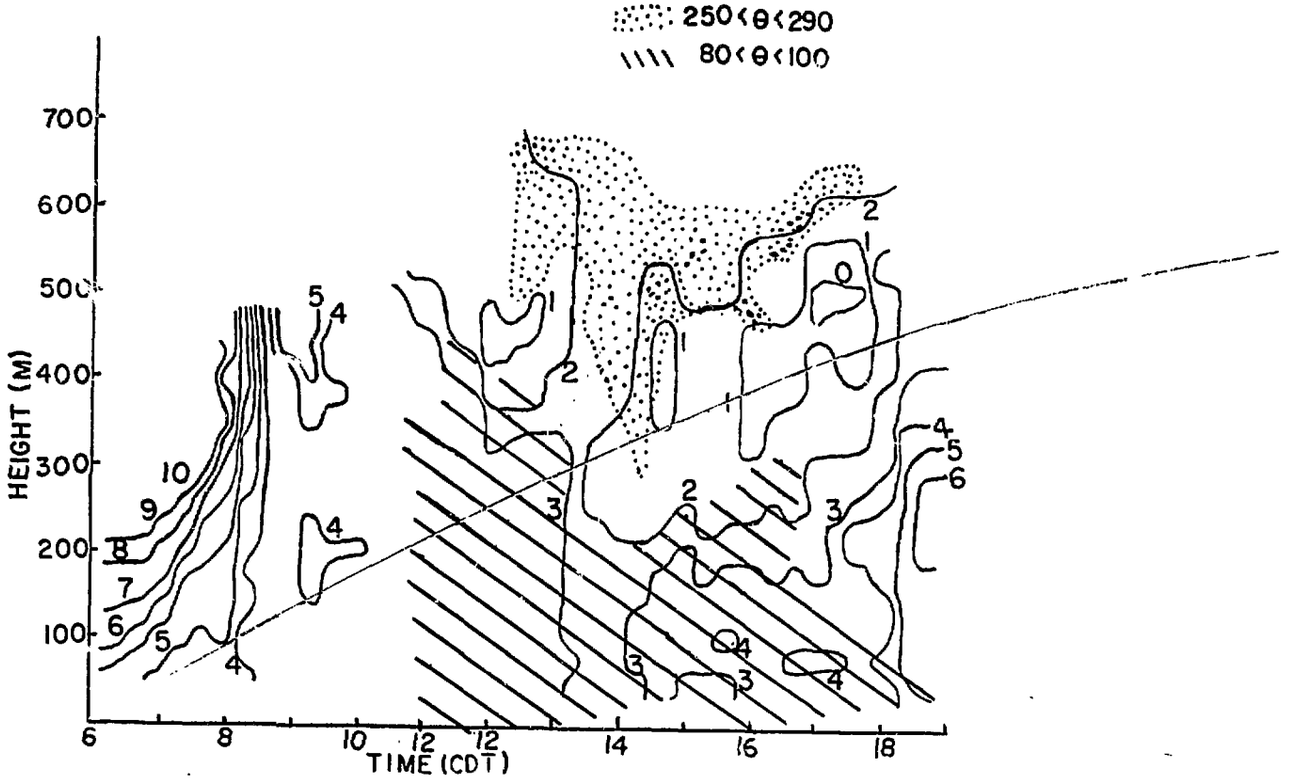

Fig. 3. Contours of wind speed and direction on 8 June 1982 derived from sodar and tethersonde data taken at the land site during the SEADEX experiment. Wind speed contours are expressed with units of meters per second.

TRACER STUDIES OF POLLUTANT DISPERSION IN A STREET CANYON

F. T. DePaul and C.-M. Sheih

Pollutant transport and dispersion in an urban street canyon when the ambient wind direction aloft is perpendicular to the canyon have been studied with use of an inert gas tracer. All measurements were taken in downtown Chicago at a street canyon 80 m long, 33.5 m high, and 24.5 m wide. Sulfur hexafluoride (SF_6) was chosen to simulate the pollutant source because there is minimal interference from background sources, SF_6 can be accurately measured at concentrations of parts per trillion (PPT), and emission rates can be easily controlled. The gas concentrations were measured by electron-capture detection following use of a gas chromatograph equipped with a 20-Å molecular sieve for gas-phase separation.

Meteorological measurements for mean ambient wind speed (U_a), wind direction (θ), and local friction velocity (u_*) were taken at 3 m above the upwind rooftop near the building edge. Ten-minute averages for U_a and u_* were obtained from a hot wire anemometer. Alignment problems usually associated with the hot wire were corrected by analyzing the data with reference to a plane where the mean vertical wind component $\bar{w} = 0$. The wind direction was measured with a wind vane.

To simulate a pollutant line source within the canyon, the SF_6 tracer was released continuously at ground level from tubing vented by a series of critical orifices spaced uniformly at 1-m intervals. Ten-minute integrated concentrations of the tracer were measured at each location in the sampling array depicted in Figure 1. These samples were collected by constant-flow pumps and stored in 5-liter Mylar bags. Concentration decay was determined by turning off the source and taking concentration measurements nearly instantaneous at about 30-s intervals.

Normalized concentration vertical profiles for sampling locations 4-7 during equilibrium conditions are shown in Figure 2. The profiles describe the relative SF_6 concentrations in the canyon and indicate a rapid reduction in concentration with height. Also shown are the average concentration profiles for samplers 10-12. These profiles indicate a significant gradient near the downwind building edge. Sampling locations 2,3,4, and 8 were used to

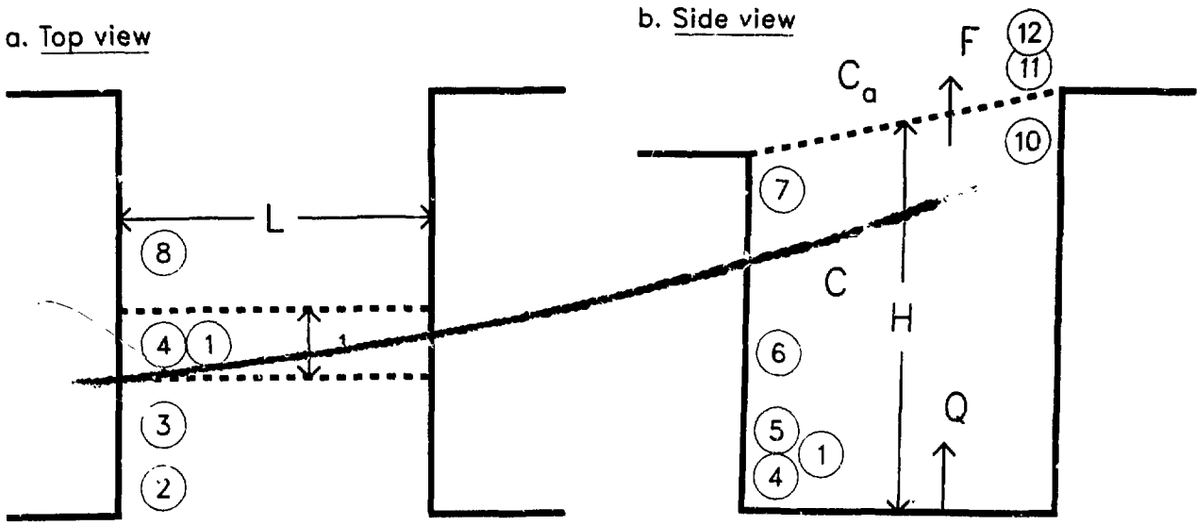

Fig. 1. Configuration of the street canyon showing location of sampling stations as indicated by circles and the controlled volume used in the analysis as indicated by the dashed lines.

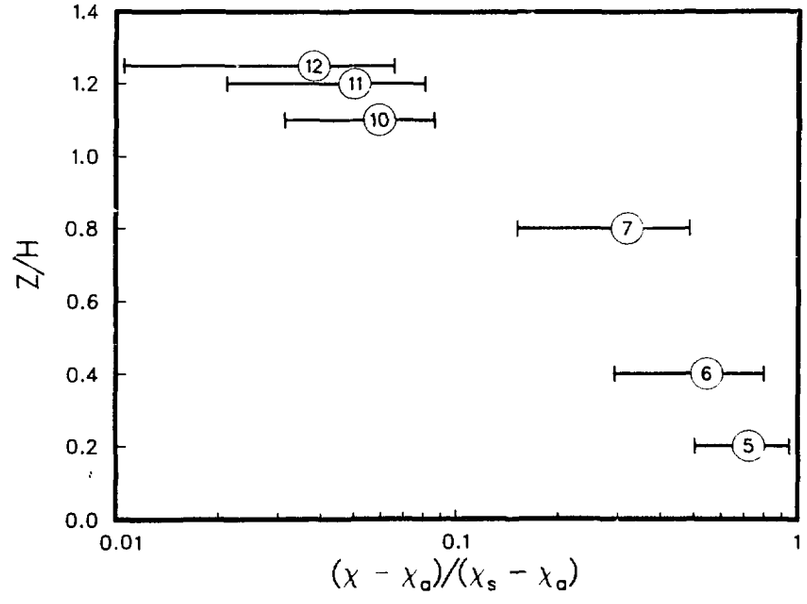

Fig. 2. The normalized vertical concentration profiles for samplers 5-7 and 10-12. The error bars indicate standard deviations.

ensure a two-dimensional profile, i.e., zero concentration gradient in the downstreet direction.

The measurements of concentration decay were used to parameterize the flux of pollutant dispersed out of the street canyon. Briefly, the budget equation of a pollutant can be expressed by:

$$d(C - Ca)/dt = Q - F \ , \tag{1}$$

where C and Ca are bulk average pollutant concentrations inside and outside the street canyon, respectively, t is time, Q is emission rate, and F is the pollutant flux out of the street canyon. Since the emission rate is often known, the pollutant concentration can be predicted with Eq. (1) if the flux can be parameterized.

Following the concept of deposition velocity commonly used in studies of surface deposition, one can introduce a bulk average ventilation velocity V_v and represent the flux term by:

$$F = (V_v/H)\ (C - C_a) \ , \tag{2}$$

where H is the height of the building. The ventilation velocity can be measured by turning off the emission source and studying the evolution of the concentration as a function of time. Setting Q = 0 and substituting Eq. (2) into Eq. (1) and then integrating the equation, one obtains the following:

$$[C(t) - C_a]/[C(0) - C_a] = \exp\ [-(V_v/H)\ t] \ , \tag{3}$$

where C(t) and C(0) are concentrations at times t and 0, and $\tau = H\ V_v^{-1}$ is a retention time or a decay time constant. The experimental results show that Eq. (3) describes very well the time evolution of the pollutant concentration. Our previous theoretical studies suggest that an approximate representation of the ventilation velocity can be:

$$V_v/u_* \sim \alpha_1 + \alpha_2\ Re \ , \tag{4}$$

where α_1 and α_2 are constants and $Re = U_a L/\nu$ is a Reynolds number based upon ambient mean wind velocity U_a, street canyon width L, and an arbitrary constant diffusivity, here taken to be the kinematic viscosity ν. The results in Figure 3 can be approximated by:

$$V_v/u_* = 0.34 + 2.03\times10^{-7}\ Re\ . \qquad (5)$$

The generality of the result given by Eq. (5) is greatly limited for several reasons. First, u_* is measured locally above an upwind rooftop and thus has values that are probably not highly representative of the mixing and flow region in the overall area upwind of the canyon. Second, the use of ν for diffusivity representative of the mixing created in the wake of the upper edge of the upwind building is clearly incorrect (because viscous mixing is insignificant in comparison to turbulent mixing above the street canyon). Finally, a different aspect ratio (L/H) might produce a vortex flow structure quite different from that in the canyon studied and thus possibly greatly alter the ventilation velocity V_v. Nevertheless, these studies give a realistic appraisal of exchange between a certain type of street canyon and the atmosphere above, and hence provide a benchmark for evaluation of the results of various physical and numerical simulations.

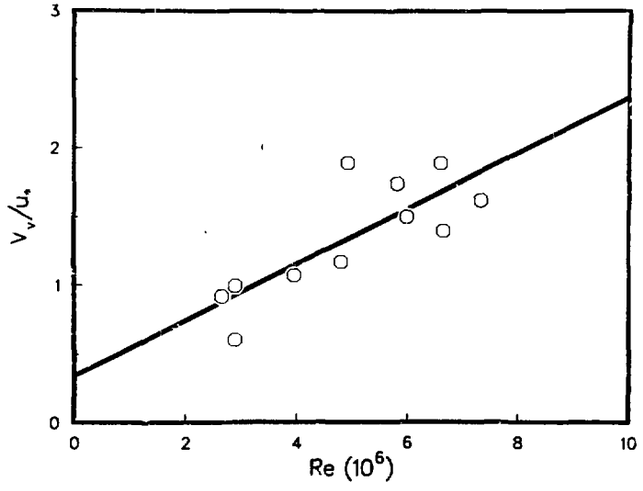

Fig. 3. The measured normalized ventilation velocity V_v/u_* as a function of a Reynolds number Re for the canyon.

EXPERIMENTAL STUDIES OF AEROSOL SIZE DISTRIBUTION IN A STREET CANYON

F. T. DePaul and C.-M. Sheih

Aerosol size distributions have been measured in a city street canyon with moderate traffic density in order to characterize the local aerosol and to determine the size fraction of aerosol transported from local sources within the canyon to the flow region aloft. The street canyon examined was one block (80 m) long, and each side was ten stories (~ 34 m) high. Instrumentation consisted of two electrical aerosol analyzers (EAA) for counting particles with diameters of 0.006 to 1 μm and an optical particle counter (OPC) for diameters of approximately 0.3 to 20 μm. The EAAs were coupled to operate simultaneously at staggered size classifications in order to avoid errors that could result if one were to assume no temporal variation in concentration between successive channels.

Typical volume-weighted particle size spectra observed in the street canyon have double modes peaked at around 0.2 μm and 10 μm. It appears that particles in the size range of 0.1-0.5 μm are the dominant submicron aerosol generated in the canyon. This is illustrated in Figure 1, which shows plots of the size spectra of average aerosol concentrations in (1) samples taken at street level within the canyon, in (2) samples taken at the upwind roof level, and (3) the difference between the two sampling levels. Averaged vertical profiles of aerosol concentration in the canyon that were obtained with the OPC exhibit a constant size distribution for particles with diameters larger than 1 μm at heights greater than 5 m.

To estimate the time required for submicron aerosol of specified size ranges to be transported from street level to roof level, simultaneous measurements of particle concentration were taken 3 m from the leeward edge of the building at both street and roof levels. The EAAs were operated at the same size classification channel and the cross-correlation coefficients of the two signals were computed for various time lags. The transport times for various particle sizes were estimated from the peaks of the correlation coefficients shown in Figure 2. The transport times for the submicron particles were found to be 12-24 s for wind speeds between 1-4 m s^{-1}, implying 1.3-2.5 m s^{-1} vertical transport winds.

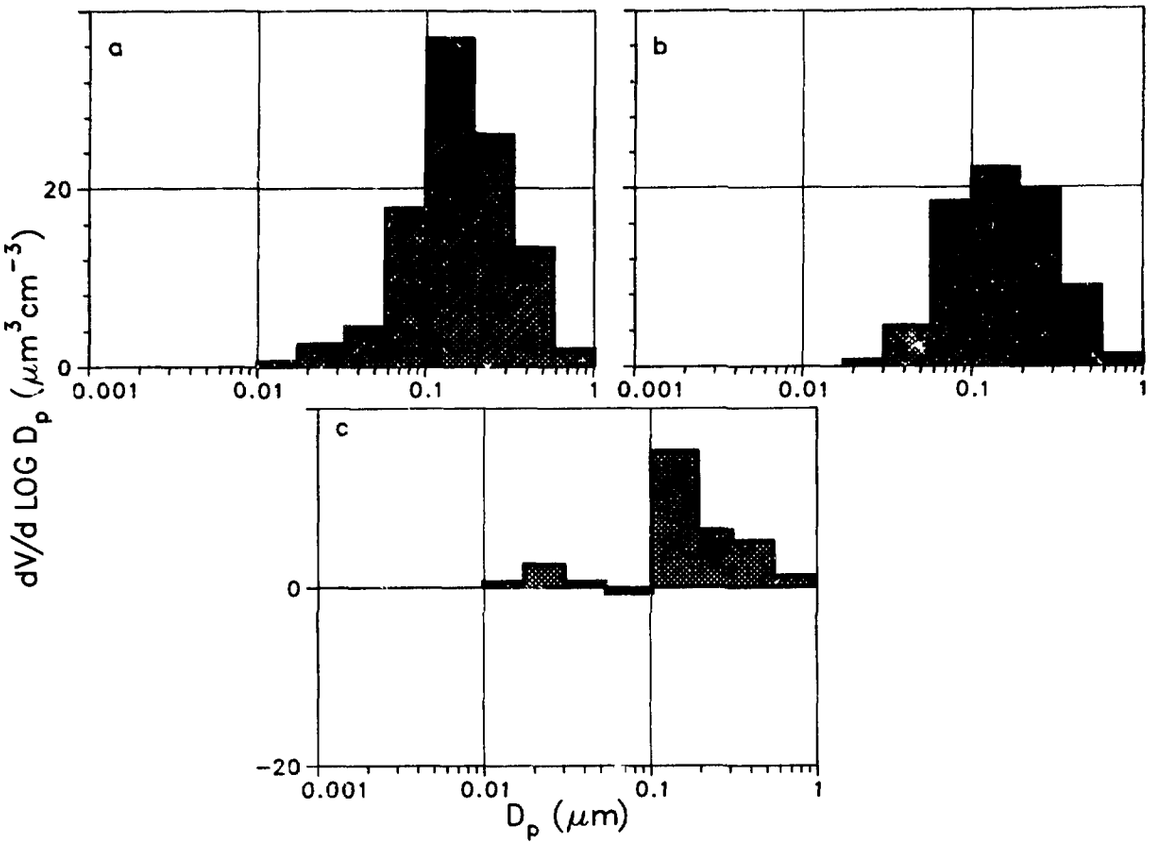

Fig. 1. Submicron aerosol size distribution for (a) spatial average concentration within the canyon, (b) upwind roof-level concentration, and (c) difference in concentration between (a) and (b).

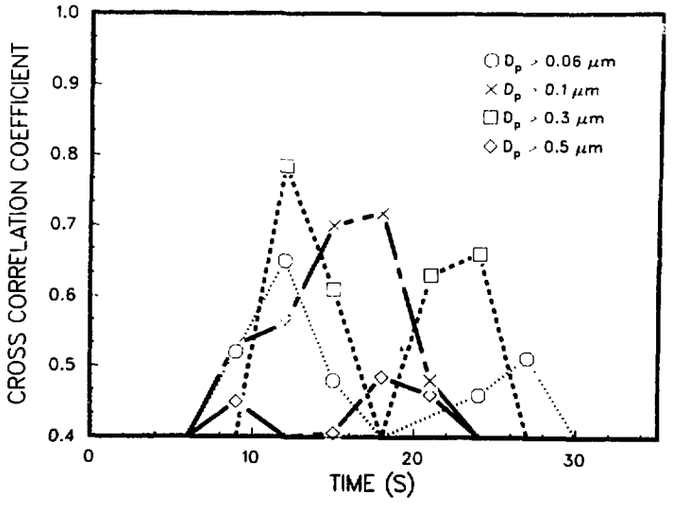

Fig. 2. Cross correlation coefficient vs. transport time for specified particle diameters (D_p).

OBSERVATIONS OF FINE PARTICLE BEHAVIOR AFFECTED BY PRECIPITATION EVENTS

S. A. Johnson*, D. L. Sisterson, and R. Kumar*

In an effort to examine the relationships between local atmospheric aerosol properties and precipitation scavenging, a modified Lundgen cascade impactor was used to sample ambient aerosols before, during, and after precipitation events. The precipitation was sampled using a standard wet/dry collector at ANL's deposition monitoring site (e.g., Sisterson and Wurfel, 1980). The chemical composition and mass loading (dry weight) of ambient submicron aerosol particles (0.3-1.0 μm aerodynamic diameter) were determined during 25 individual precipitation events over a 12-month period. Chemical analyses were carried out with Fourier-transform infrared absorption spectroscopy for the fine-particle aerosols and with established wet-chemical analyses (e.g., Sisterson and Wagner, 1980) for the precipitation samples. The meteorological and limited air-quality data collected for each precipitation event were examined to investigate the factors responsible for the observed behavior of the aerosol particles. In this report, only the variations in aerosol mass and chemistry in relation to specific precipitation events are discussed.

In several cases where the precipitation was not accompanied by a frontal passage or other means of change in type of air mass, two cases of fine-particle aerosol behavior were observed. In one, the concentration of aerosol particles was reduced during rain, but the concentration recovered quickly after the event. In the other, the aerosol particle concentrations increased during the rain. While the ammonium sulfate content of the aerosols was also affected by the precipitation, the changes were not always similar to those observed in the total particle mass loading.

The first case is a decrease in aerosol mass loading during precipitation, followed by recovery. In almost every occurrence of this nature, the decrease in mass loading could be attributed to precipitation scavenging of local particles, and subsequent recovery due to advection of non-scavenged air

*Environmental Chemistry Group, Chemical Technology Division.

within the same air mass to the sampling location. Scattered thunderstorm activity, for example, would usually produce behavior of this nature.

Examples of the second case, an increase in the particle concentration during the precipitation, are shown in Figure 1. Of the various factors that could be correlated with such behavior (local plume being swept in and out of the sampling site during precipitation, etc.), one that was very often found was an increase of relative humidity from less than 50% to greater than 80% (usually near 100%). Such a change in humidity can lead to the growth of particles smaller than 0.3 μm to a size between 0.3 and 1.0 μm (Radke et al., 1980). Thus, the apparent increases in particle mass loading were probably

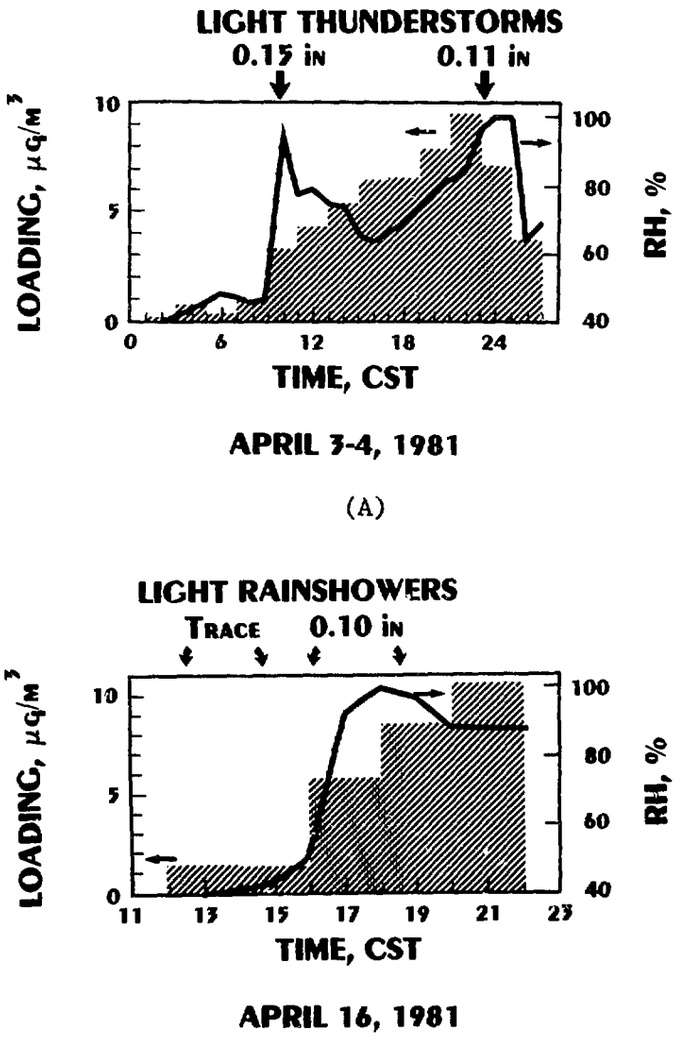

Fig. 1. Examples of particle mass loading (0.3-1.0 μm aerodynamic diameter and indicated by diagonal hatching) that increased during precipitation (vertical hatching) when the relative humidity (solid line) increased from near 50% to near 100% for (A) during light thunderstorms and (B) during light rain showers.

not due to an increase in the number of particles, but rather were due to a shift in the particle-size distribution. It should be noted that humidities remained essentially constant before, during, and after precipitation for the first case of particle behavior; i.e., a decrease in aerosol mass loading during precipitation accompanied by recovery. Thus, in many cases relative humidity apparently can affect particle loading more strongly than precipitation scavenging.

Finally, in some cases, a decrease in ammonium sulfate particles simultaneous with an increase in particle mass loading was observed. The reasons for such behavior are not fully understood. A possible explanation is that the observed changes were caused by a combination of particle scavenging and advection of new particles from local sources due to slight changes in wind direction that occured during the rain. The meteorological data, although showing a gradual shift in the wind direction during precipitation, do not conclusively support this argument.

References

Radke, L. F., P. V. Hobbs, and M. W. Eltgoth, 1980: Scavenging of aerosol particles by precipitation. J. Appl. Meteorol. 19, 715-722.

Sisterson, D. L. and D. Wagner, 1980: A comparison of the chemistry of event and weekly precipipation samples in northern Illinois--A preliminary report, Part 2, Argonne National Laboratory Radiological and Environmental Research Division Annual Report, ANL-80-115, Part IV, pp. 72-74.

Sisterson, D. L. and B. Wurfel, 1980: A comparison of the acidity of event and weekly precipitation samples in northern Illinois--A preliminary report, Part 1, Argonne National Laboratory Radiologcal and Environmental Reseach Division Annual Report, ANL-80-115, Part IV, pp. 68-71.

DETERMINATION OF OUTLIERS IN THE WEEKLY-VERSUS-EVENT PRECIPITATION CHEMISTRY STUDY

D. L. Sisterson

An objective method for the determination and elimination of outliers in the weekly-versus-event precipitation chemistry study is necessary to ensure that the quality of data used is high. The experimental procedures for the collection and chemical analysis of weekly precipitation-weighted sums of event samples by Argonne National Laboratory (ANL) for comparison over a two-year period with weekly precipitation samples analyzed by the National Atmospheric Deposition Program (NADP) have been discussed elsewhere (Sisterson and Wurfel, 1980). Samples affected by collector malfunction or obvious contamination (bird excrement, etc.) were not included in the data set. Outliers were found by scrutinizing the data with regard to ion balance, sample completeness, and statistical determination of ANL/NADP pairs that showed unusually large difference in chemical concentrations of ionic species.

When the ion balance (expressed in percent as 100 x ([A] - [C])/([A] + [C]), where [A] and [C] are the sums of all anion and cation concentrations, respectively) of an ANL sample exceeded ±14%, the sample was reanalyzed. This limit of 14% is similar to that used in application of quality assurance procedures by the National Atmospheric Deposition Program, which results in 10% of their samples being reanalyzed. Rarely were the ion balances of the ANL event samples worse than 20% and, on several occasions, the reanalysis showed no significant change in ion balance. Analytical procedure did not appear to be the cause of the large ion balances in those cases, so it was assumed initially that other species, most likey organic, were present. Since only inorganic species were investigated, samples that still had larger ion balances after reanalysis were included in the data base. For samples with acceptable ion balances after reanalysis, the reanalyzed ion-concentration values were included in the data base.

The ANL samples collected during the two-year period usually consisted of several single event samples, some of which had liquid volumes less than the amount required for complete field and chemical analyses. Since chemical

analysis of all event samples contributing to an ANL sample was occasionally incomplete, pseudoconcentrations of the small-volume event sample were computed (but not used in the final averaging) by assuming that for each ion the NADP sample and the ANL precipitation-weighted concentrations were equal. If any one of the computed ion pseudoconcentrations of the small-volume sample was more than 10 times greater the highest concentrations found for that ion during the two-year period (which included laboratory analysis of some samples of 20 ml), the ANL sample was eliminated from the data base. This was a conservative procedure because the trend throughout the two-year intercomparison study was for NADP ion concentrations (except $[H^+]$, $[K^+]$, and $[NH_4^+]$) to be greater than ANL ion concentrations. Five of the 12 incomplete ANL samples over the two-year study period were eliminated in this manner.

It was noticed that acceptable incomplete ANL samples occurred when the precipitation amount of the unanalyzed event sample was less than about 2.5% of the weekly total sample amount. In other words, the screening method used apparently results in incomplete ANL samples being classed as acceptable when only very small sample amounts are missing. Since ion concentration tends to be related inversely to precipitation amount, the events with very small liquid amounts may have large ion concentrations. To a first approximation, however, an ion concentration of an event sample with a volume of only 2.5% or less of the total for the week would have to be larger than 10 times the highest individual ion concentration observed to make a significant contribution to the weekly total ion concentration. Hence, from the few cases of incomplete ANL samples studied, it appears appropriate to reject ANL samples from the data base if an unanalyzed event sample represents more than 2.5% of total precipitation amount for that week. This is not expected to be universally true.

A least squares regression (Prahl, 1981a,b) was used on the surviving ANL and NADP individual ion-concentration pairs to detemine a best-fit line and standard deviation. The pairs were plotted (see, for example, Fig. 1) and any pair that fell outside of $\pm 3\sigma$ was considered an outlier. The pair was carefully reviewed for individual event or weekly samples with poor ion balances (greater than ±14%), for incompleteness in ANL samples (although initially accepted), and field notes that might indicate a problem in analysis or storage that was not severe enough to initally eliminate the sample from the

data base. If one of more of these problems were found, the the outlier pair for a particular ion was eliminated from the data base. If the sample pair was an outlier for a significant number of ions, it was eliminated from the data base. Outlier pairs were not eliminated from the data set if no reasonable cause could be found to warrant removal.

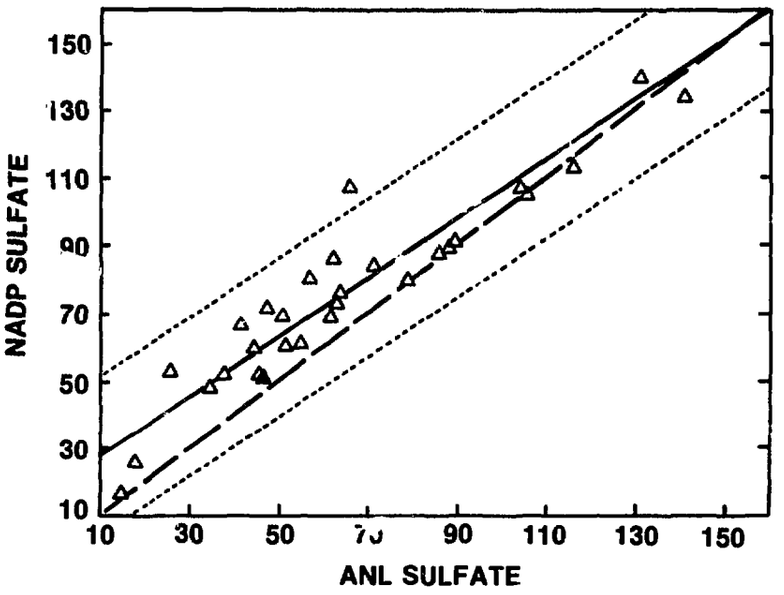

Fig. 1. Weekly (NADP) versus event-summed (ANL) sulfate ion concentrations for samples collected from April 1980 to March 1981. The heavy dashed line represents a slope of 1, the solid line is the least squares regression, and the dotted line represents $\pm 3\sigma$.

References

Prahl, W. H., 1981a: Fitting linear equations to sets of experimental data, Chemical Engineering, 10 August 1981, pp. 85-88.

Prahl, W. H., 1981b: Further note on fitting linear equations to sets of experimental data, Chemical Engineering, 5 October 1981, p. 5.

Sisterson, D. L. and B. Wurfel, 1980: A comparison of acidity of event and weekly precipitation samples in northern Illinois--A preliminary report, Part 1, Argonne National Laboratory Radiological and Environmental Research Division Annual Report, ANL-80-115, pp. 68-71.

URBAN INFLUENCES ON LOCAL PRECIPITATION CHEMISTRY DURING WINTER AND SPRING

D. L. Sisterson

Precipitation samples collected at Chicago's lakefront and at Argonne National Laboratory (~ 40 km SW) during the period June 1981 through May 1982 were analyzed to investigate urban influences on local precipitation chemistry. The Argonne (ANL) and Chicago (CHI) sample pairs were stratified according to wind direction, and wet deposition values normalized by precipitation amount were used in the comparison to minimize some of the potential effects of spatial variability of convective and stratiform storms. Experimental procedures and the results of the first half, or summer and fall (June-November 1981) of the study period are discussed elsewhere (Sisterson, 1981a). This report characterizes the 16 pairs of weekly samples that were collected through the second half, or winter and spring (December 1981 - May 1982) of the study period.

Most of the winter and spring precipitation amounts were atypically small; therefore weekly sampling procedures were employed instead of the event sampling procedures used during the summer and spring. Thus, at both sites a number of events could usually provide a precipitation amount sufficient for chemical analysis. There may be some differences in comparing the winter and spring weekly concentrations to the summer and fall summed event values (Sisterson and Wurfel, 1981), but the differences are considered inconsequential in comparison to urban influences.

As before (Sisterson, 1981a), the ANL and CHI sample pairs were stratified according to the wind direction that existed prior to each of the events. Only weekly samples for which wind directions prior to all precipitation events were from the same quadrant were used in the comparison; just one weekly sample was eliminated by application of this criterion.

Normalized total wet deposition values (actually concentration averages weighted by precipitation amount for each wind quadrant) of ANL and CHI samples are shown sorted by wind direction quadrant in Table 1. There were no samples collected for the northwest quadrant. Differences between the ANL and CHI normalized wet deposition values are shown in Table 2. The variations and differences in these tables might not accurately quantify the influence of

Table 1. Normalized total wet deposition values for chemical species analyzed in Argonne (ANL) and Chicago (CHI) rain samples stratified by wind quadrants. All values are μeq/L except where indicated.

Quadrant	ANL	CHI	ANL	CHI	ANL	CHI
	H^+(lab pH)		Rain, g x 10^3		Ca^{+2}	
SW (5)*	87.4	31.5	1.34	0.40	19.4	63.7
SE (8)	82.8	77.2	7.20	7.63	18.5	26.1
NE (3)	82.1	79.6	3.08	3.50	20.0	25.2
	Mg^{+2}		Na^+		NH_4^+	
SW (5)	8.9	19.2	4.0	12.0	50.6	55.6
SE (8)	8.9	9.0	6.3	7.7	41.4	42.8
NE (3)	6.3	7.3	10.6	11.1	58.9	72.9
	NO_3^-		Cl^-		SO_4^{-2}	
SW (5)	42.8	49.4	3.2	13.3	61.4	83.4
SE (8)	28.0	33.2	3.8	8.3	61.2	67.5
NE (3)	40.0	51.4	8.2	9.7	68.3	81.0

* The number of weekly samples collected for each quadrant is given in parenthesis.

local emissions in Chicago on precipitation chemistry, but the trends are probably representative of an urban influence.

Generally, CHI samples for the winter-spring period have higher normalized total wet deposition values for each chemical species except H^+, regardless of wind direction. A similar result was found in the summer-fall half of the study. The normalized total wet deposition values for nearly all chemical species analyzed, however, do not show significant variation by wind direction as before. Precipitation collected during the winter-spring period was nearly all from stratiform clouds, not convective as during the summer-fall half of the study, and would reflect more exclusively the local scavenging of pollutants. However, precipitation periods are much longer for stratiform systems, with varying wind direction, and this condition tends to obscure the effects of local emissions with regard to wind direction.

Table 2. Percent difference [(CHI-ANL)/mean] x 100% between Argonne (ANL) and Chicago (CHI) normalized total wet deposition values in Table 1 according to wind quadrant.

Quadrant	H^+(lab pH)	Rain	Ca^{+2}
SW (5)*	-94.0	-106.7	+106.7
SE (8)	-7.1	+5.8	+34.0
NE (3)	-3.0	+12.7	+23.1
	Mg^{+2}	Na^+	NH_4^+
SW (5)	+100.0	+101.1	+9.3
SE (8)	+1.0	+20.1	+3.3
NE (3)	+14.8	+4.5	+21.3
	NO_3^-	Cl^-	SO_4^{-2}
SW (5)	+14.5	+121.8	+30.4
SE (8)	+16.8	+75.1	+9.8
NE (3)	+24.8	+16.7	+17.0

* The number of weekly samples collected for each quadrant is given in parenthesis.

The soil-derived components (Ca^{+2}, Mg^{+2}, etc.) are significantly larger at both sites during the winter-spring half of the study. The samples were collected during seasons that have increased synoptic winds; in this case, unusually little snow cover and rainfall occurred. The greater strength of winds and lack of snow cover on soils would likely contribute to increased wintertime soil-particle loading. The increased winter-spring Na^+ and Cl^- values might be a result of salting for icy road conditions, even though both collection sites are far removed from busy roadways.

The SO_4^{-2}, NO_3^-, and NH_4^+ concentrations at both sites are also greater during the winter-spring period, which is somewhat surprising because the prevelant stratiform systems can be characterized by the less efficient sub-cloud scavenging processes of pollutants in comparison to convective systems. Nevertheless, stratiform systems are usually associated with lesser precipitation intensity than convective storms, and concentrations of pollutants in precipitation generally increase with decreasing precipitation intensity.

Regardless of season or wind direction, the CHI samples generally have larger concentrations of all ions except of H^+. While Chicago precipitation samples may well reflect the higher urban concentrations of airborne pollutants, the pH of that precipitation is higher than suburban-rural Argonne. Apparently, there is a disproportional increase of Ca^{+2}, Mg^{+2}, and NH_4^+ that offsets acidifying species (Sisterson, 1981b), resulting in lower acidities in the urban area.

References

Sisterson, D. L., 1981a: Effects of Chicago emissions on local precipitation chemistry--A preliminary report, Argonne National Laboratory Radiological and Environmental Research Division Annual Report, ANL-81-85, Part IV, pp. 91-94.

Sisterson, D. L., 1981b: Partial neutralization of rainfall acidity by soil derived particles in northeastern Illinois, Argonne National Laboratory Radiological and Environmental Research Division Annual Report, ANL-81-85, Part IV, pp. 73-77.

Sisterson, D. L. and B. Wurfel, 1981: Seasonal and annual comparison of weekly and event sampling of precipitation chemistry. Argonne National Laboratory Radiological and Environmental Research Division Annual Report, ANL-81-85, Part IV, pp. 69-72.

INDICATIONS OF NONLINEARITIES IN PROCESSES OF WET DEPOSITION

I.-Y. Lee and J. D. Shannon

The relationship between man-made pollutant emissions and the deposition of acidic or acidifying pollutants is not well understood. The evaluation of trends in precipitation chemistry frequently gives ambiguous results because of irregular sampling procedures, meteorological variations from one study period to the next, and changes in laboratory analysis procedures. An example of this is that the observed sulfate deposition trend in western Europe does not clearly reflect a known increase in sulfur emissions (Granat, 1978). This nonlinear response has been attributed by Granat to factors other than sampling or chemical analysis procedures,--namely, to increased deposition in areas east of the network in association with a change in the prevailing circulation pattern. An alternative explanation for this may be found in clear-air and in-cloud chemistry, since the conversions of SO_x and NO_x gases to sulfate and nitrate can compete if oxidants, e.g., OH radical, are limited. In this respect, the European data, which show increasing deposition of nitrate, could be interpreted to indicate that NO_x is more effectively oxidized and deposited by wet processes near the source regions than SO_x.

To examine North American data, the profiles of concentration of relevant chemical species in precipitation at MAP3S sites along a cross section connecting locations at 45°N, 75°W and at 40°N, 85°W are presented in Figure 1 (MAP3S/RAINE Research Community, 1982). The orientation of the cross section was chosen on the basis that the wet deposition of pollutants (and water) over the northeastern United States is mainly associated with flow from the southwest (Wilson et al., 1982). The data points from the coastal MAP3S sites at Lewes, Delaware, and Brookhaven, New York, indicated in Figure 1 are excluded from the present analysis. Here we see that the sulfate/nitrate ratio is greater than 1 over the major source regions, and this approximately reflects the ratio of SO_x to NO_x from anthropogenic emissions on a molar basis. This seems to contradict preferential oxidation and wet deposition of NO_x. Numerical simulations have been carried out with a model consisting of clear-air chemistry (Lee, 1983a) and in-cloud chemical reactions (Lee, 1983b) in order to examine chemical factors (e.g., the molar ratio of sulfate to

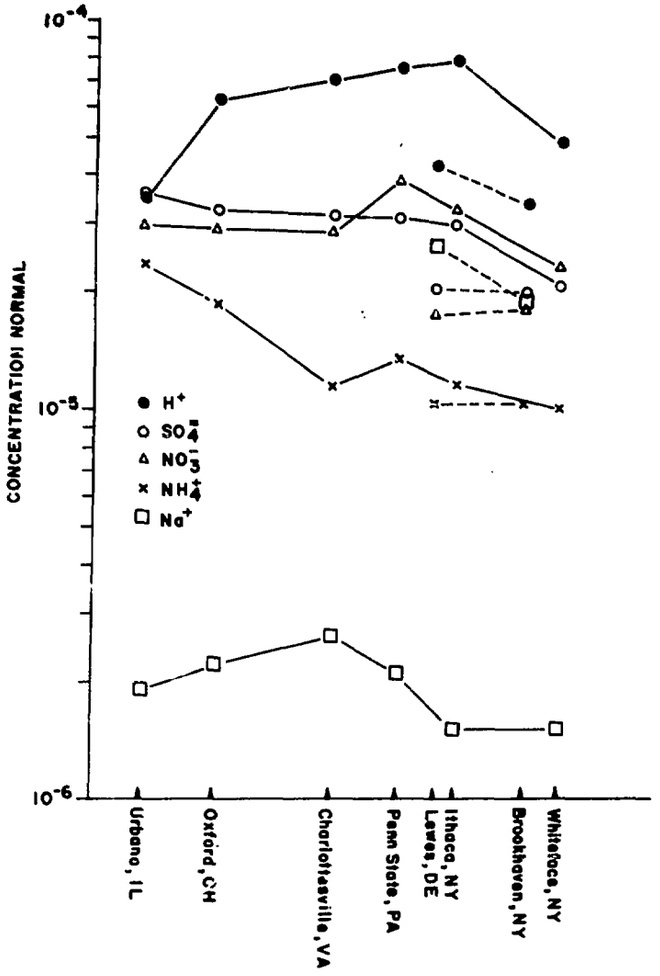

Fig. 1. Cross-sectional depiction of MAP3S precipitation chemistry data.

nitrate in precipitation) that can be used as indicators of the extent of nonlinear processes.

Nonlinear processes in precipitation scavenging are most likely to be important close to sources where sulfur and nitrogen oxides exist at relatively high concentrations. With high concentrations, the processes of conversion to sulfate and nitrate in precipitation might be self-limiting or limited by insufficient amounts of reactive substances in the environment.

Computer model runs I, II, III and IV were designed to study the relationship between ambient concentrations of SO_2 and NO_2 and concentrations of $SO_4^=$ and NO_3^- in the cloud water. For these runs, the liquid water mixing ratios were specified. The initial concentrations of SO_2 and NO_2, respectively, in clear air were 5 and 10 ppb for Run I, both 10 ppb for

Run II, 15 and 10 ppb for Run III, and 20 and 10 ppb for Run IV. With these different initial values, the clear-air chemistry model was used to compute the temporal variations of gaseous concentrations of precursor species and sulfate mixing ratios in aerosols for input to in-cloud chemical processes.

Aerosols serve as condensation nuclei during the cloud formation. The monthly variations of sulfate content in air and of $SO_4^{=}$ and NO_3^- concentrations in precipitation obtained from Canadian precipitation chemistry data in the Toronto area in Figure 2 (Niemann, 1982) are presented. The sulfate concentrations in precipitation do not appear to be well correlated with the atmospheric concentration of sulfate. This may result in part from the fact that the monthly average atmospheric concentration of sulfate may not accurately represent the concentration during the episodic precipitation events.

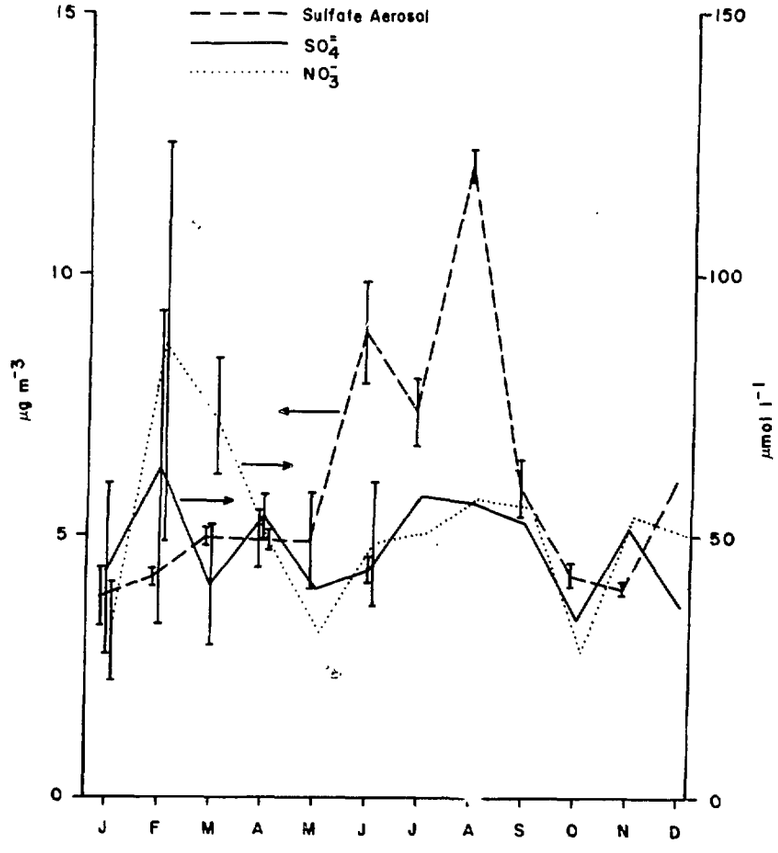

Fig. 2. Monthly variations of sulfate content in ambient aerosol and of sulfate and nitrate concentrations in precipitation near Toronto.

Although the production of sulfate particles increases during the summer months, only particles with diameters greater than about 0.1 μm can be activated to form cloud droplets, because as smaller particles, which form mainly from SO_2 by physical and chemical transformation processes (Lee, 1983a), are not activated. In this respect, sensitivity studies have been carried out for cases when all the sulfates serve as cloud condensation nuclei (Model A) and for cases when the total mass density of active aerosol particles is invariant (Model B). For the latter cases, the sulfate aerosol properties are assumed to have the same values as in the case of Run II. We also assume in all cases that the nitrate content in aerosols is one order of magnitude smaller than the sulfate content. Observations of chemical composition of aerosols show that the nitrate content in aerosols is, in fact, quite small (Ohta et al., 1981; Hobbs and Hegg, 1982).

Results from the four runs and annual mean values of Canadian precipitation chemistry data in the Toronto area are summarized in Table 1. As described above, Runs I through IV were designed to examine the relationships between pollutant precursors and corresponding acidic species in wet deposition. In general, both simulations and precipitation chemistry data show that the molar ratio $SO_4^=/NO_3^-$ is approximately 1. The initial values for SO_2/NO_2 vary between 0.5 and 2.0; the corresponding ratios obtained after 16 hours of real time simulation with the clear-air chemistry model (conducted to obtain a steady state spectrum of aerosol particles) vary between 0.6 and 2.7. This indicates that the mean clear-air transformation rate of SO_2 is smaller than that of NO_2, and that the SO_2/NO_2 ratio becomes larger far downwind from the source, if dry and wet removal rates are similar for the two species. The simulation also indicates that the molar ratio $SO_4^=/NO_3^-$ in cloud water increases as the ratio SO_2/NO_2 increases. However, we see clearly that the relationship between the increase of precursor SO_2/NO_2 and the increase of $SO_4^=/NO_3^-$ in cloud water is nonlinear on the scale examined, and that the degree of this nonlinear response becomes more significant for cases when the total mass density of the cloud condensation nuclei in air is assumed to be invariant (Model B). This nonlinear response can also be seen in the pH values. The cloud water pH decreases slowly with increasing input ratio SO_2/NO_2 for a given value Q of liquid water mixing ratio, and increases slowly with increasing Q when the ratio SO_2/NO_2 is fixed.

Table 1. Comparison of annual mean precipitation chemistry data with computed values.

	Initial			Precursor				Model A			Model B		
	SO_2 (ppb)	NO_2 (ppb)	SO_2/NO_2	SO_2 (ppb)	NO_2 (ppb)	SO_2/NO_2	Q (g kg^{-1})	$SO_4^{=}$ ($\mu mol\,l^{-1}$)	$SO_4^{=}/NO_3^{-}$	pH	$SO_4^{=}$ ($\mu mol\,l^{-1}$)	$SO_4^{=}/NO_3^{-}$	pH
RUN I	5	10	0.5	4.7	7.4	0.6	0.5	66.7	0.73	3.97	78.5	0.86	3.92
							1.0	34.4	0.75	4.25	40.3	0.88	4.21
							1.5	24.0	0.79	4.42	27.9	0.91	4.37
							2.0	19.0	0.83	4.52	21.9	0.96	4.48
RUN II	10	10	1.0	9.7	7.3	1.3	0.5	79.0	0.86	3.87			
							1.0	41.1	0.90	4.16			
							1.5	29.1	0.95	4.32			
							2.0	23.4	1.02	4.42			
RUN III	15	10	1.5	14.4	7.2	2.0	0.5	90.9	0.99	3.79	79.3	0.87	3.82
							1.0	47.5	1.04	4.08	41.7	0.91	4.11
							1.5	33.8	1.11	4.24	29.9	0.98	4.27
							2.0	27.4	1.20	4.34	24.4	1.07	4.37
RUN IV	20	10	2.0	19.1	7.0	2.7	0.5	102.7	1.12	3.73	79.5	0.87	3.79
							1.0	54.0	1.18	4.02	42.2	0.92	4.08
							1.5	38.5	1.26	4.18	30.6	1.00	4.23
							2.0	31.1	1.36	4.28	25.2	1.10	4.33
Observed											47.7 ±0.9	0.99 ±0.24	4.29 ±0.23

References

Granat, L. 1978: Sulfate in precipitation as observed by the European atmosphere chemistry network, Atmos. Environ. 12, 413-424.

Hobbs, P. V. and D. A. Hegg, 1982: Sulfate and nitrate mass distribution in the near fields of some coal-fired power plants, Atmos. Environ. 16, 2657-2662.

Lee, I.-Y., 1983a: Formation of sulfate in cloud-free environment, J. Appl. Meteorol. 22, 163-170.

Lee, I.-Y. 1983b: Effects of cloud dynamics on cloud-water acidification, This report.

MAP3S/RAINE Research Community, 1982: The MAP3S/RAINE precipitation chemistry network: Statistical overview for the period 1976-1980, Atmos. Environ. 16, 1603-1631.

Niemann, B. L., 1982: The 1980 data set for further evaluation of regional air quality/acid deposition simulation models, Unpublished Report, U. S. Environmental Protection Agency, 31 pp.

Ohta, S., T. Okita, and C. Kato, 1981: A numerical model of acidification of cloud water, J. Meteorol. Soc. Japan 59 892-901.

Wilson, J. W., V. A. Mohnen, and J. A. Kadlecek, 1982: Wet deposition variability as observed by MAP3S, Atmos. Environ. 16, 1667-1676.

EFFECTS OF CLOUD DYNAMICS ON CLOUD-WATER ACIDIFICATION

I.-Y. Lee

Numerical simulations have been carried out with a model that simulates in-cloud chemical reactions and dynamic and microphysical processes of cumulus cloud development. The in-cloud chemical processes are constructed under the assumptions that (1) the cloud droplets form on condensation nuclei whose water-soluble portion is composed of H_2SO_4, $(NH_4)_2SO_4$, and NH_4NO_3, and (2) the cloud water is in equilibrium with gas-phase chemical species of SO_2, NH_3, CO_2, and HNO_3. The aqueous chemical reactions used in this study are listed in Table 1. The chemistry set is a modified version of a model used for cloud acidification studies by Ohta et al. (1981) over Kanto, Japan.

In the present study, the production of $SO_4^=$ by $SO_3^=$ oxidation is included (Miller and dePena, 1972), but HCl gas is excluded from the gas-liquid phase reactions because of its insignificant effect on the acidification of continental clouds. The model simulations show that the amount of $SO_3^=$ produced in the cloud water by dissolution of SO_2 is approximately one order of magnitude smaller than the $SO_4^=$ produced from sulfates during the typical lifetime of a cumulus (~ 30 minutes) for pH values ranging from 3 to 5. At electro-neutrality, the hydrogen ion concentration in cloud water may be computed from the equation:

$$\left(1 + \frac{K_6K_7}{K_1} P_{NH_3}\right)[H^+]^3 - 2[SO_4^=]_a[H^+]^2 - \frac{1}{\omega_+\omega_=}\left(K_1 + K_2K_3P_{SO_2} + K_8K_9P_{CO_2}\right.$$

$$\left. + K_{11}K_{12}P_{HNO_3}\right)[H^+] - \frac{2}{\omega_+^2\omega_=}\left(K_2K_3K_4P_{SO_2} + K_8K_9K_{10}P_{CO_2}\right) = 0 \,, \qquad (1)$$

where K denotes the equilibrium constant, P the partial pressure of a corresponding gas in air, ω the activity coefficient, and $[SO_4^=]_a$ the $SO_4^=$ concentration resulting from dissolved aerosols. Since P, as well as ω, varies with the hydrogen ion concentration in the cloud water, the calculation of $[H^+]$ is computed with ω initially equal to unity; thereafter, the computation is

repeated with new values of P and ω until the relative adjustment with respect to the hydrogen ion concentration becomes less than 0.01 per iteration.

Table 1. Aqueous chemical reactions.

Reactions	Reaction Constants	Source
$H_2O \rightleftharpoons H^+ + OH^-$	k_1	Orel and Seinfield (1977)
$(SO_2)_g + H_2O \rightleftharpoons SO_2 \cdot H_2O$	k_2	Orel and Seinfield (1977)
$SO_2 \cdot H_2O \rightleftharpoons H^+ + HSO_3$	k_3	Orel and Seinfield (1977)
$HSO_3^- \rightleftharpoons H^+ + SO_3^=$	k_4	Orel and Seinfield (1977)
$SO_3^= \rightleftharpoons SO_4^=$	k_5	Miller and dePena (1972)
$(NH_3)_g + H_2O \rightleftharpoons NH_3 \cdot H_2O$	k_6	Hales and Drewers (1979)
$NH_3 \cdot H_2O \rightleftharpoons NH_4^+ + OH^-$	k_7	Orel and Seinfield (1977)
$(CO_2)_g + H_2O \rightleftharpoons CO_2 \cdot H_2O$	k_8	Orel and Seinfield (1977)
$CO_2 \cdot H_2O \rightleftharpoons H^+ + HCO_3^-$	k_9	Orel and Seinfield (1977)
$HCO_3^- \rightleftharpoons H^+ + CO_3^=$	k_{10}	Orel and Seinfield (1977)
$(HNO_3)_g + H_2O \rightleftharpoons HNO_3 \cdot H_2O$	k_{11}	Davis and deBruin (1964)
$HNO_3 \cdot H_2O \rightleftharpoons H^+ + HO_3^-$	k_{12}	Davis and deBruin (1964)

The in-cloud chemistry model is coupled with a cloud model. The cloud model represents cloudy and clear regions by two concentric air columns--an inner cylindrical column corresponding to the cloud region and an outer annular column corresponding to the surrounding clear region. Both lateral eddy mixing and dynamic entrainment of air variables are included to study the influence of changes in the environment on cloud development and vice versa (Asai and Kasahara, 1967). The combined model computes temporal changes in dynamic variables such as vertical velocity, temperature, water vapor and liquid water mixing ratios, chemical species concentrations, and aqueous

chemical variables such as pH values in the cloud water and ionic concentrations of species involved in the cloud acidification processes. The cloud model conserves the integral properties of the system of cloud plus environment such as total water substance and moist static energy.

A simple initial thermal and moisture structure is assumed in the model computations. In the subcloud layer, 0 to 1000 m, the temperature decreases dry adiabatically, reaching 20°C at 1000 m, and the mixing ratio decreases at a rate of approximately 1 g kg^{-1} km^{-1}, reaching 16 g kg^{-1} (95% relative humidity) at the cloud base. A dry inversion layer is assumed near the top of the model in order to inhibit extensive cloud development. As expected, the cloud formation and dissipation processes occur in the region between subcloud and inversion layer. In this region, the temperature in both the cloudy and clear areas decreases initially with a lapse rate of approximately 6°C km^{-1}; the relative humidity decreases by 1% per 100 m. To initiate the cloud development, a layer between 1100 and 1900 m is assumed to be saturated and to have a vertical velocity profile of the form: $w = \sin [\pi(z-1000)/1000]$ in m s^{-1}, with z in meters. The effect of the initial vertical velocity field becomes insignficant after a few minutes of cloud development.

The initial concentrations of SO_2, HNO_3, NH_3 and CO_2 are set at 8 ppb, 5 ppb, 2ppb, and 330 ppm, respectively. It is also assumed that the aerosol sulfate and nitrate concentrations are 10 and 1 μg m^{-3}, respectively, with a molar density ratio for $(NH_4)_2SO_4$ to H_2SO_4 of 0.68:0.32.

Simulations of the vertical velocity w and the liquid water mixing ratio Q show the typical dynamic characteristics associated with a fair weather cumulus. The maximum values of both w and Q are located in the upper part of the cloud, with w less than 3 m s^{-1} and Q less than 1 g kg^{-1}. The temporal and spatial variations of ambient SO_2, in-cloud SO_2, and cloud water pH are presented in Figures 1-3. The in-cloud decrease in SO_2 concentration occurs mainly in the upper part of the cloud, with a maximum of approximately 38%; while the corresponding maximum SO_2 loss in the ambient air is about 10%. The pH field shows a pattern similar to that of cloud water content and ranges between 3.1 and 4.2. The SO_2 evolution during cloud development shows quite interesting features associated with entraining and detraining air currents and with in-cloud chemical processes. One can clearly identify the reduction in the SO_2 concentration in the upper part of the cloud environment resulting

from the modification of air characteristics by detraining air currents from the cloud. Alternately, the reduction of ambient SO_2 can be understood by examining the in-cloud profile of SO_2 associated with the cloud-acidification processes. The amount of in-cloud reduction of SO_2 varies with the liquid water mixing ratio Q. However, the numerical study shows that the response between the variations of dissolved SO_2 and of Q is nonlinear and that the dilution by Q overcompensates the increase of cloud water acidity. Therefore, low acidity (high pH) corresponds to high Q values and vice versa, as shown in Figure 3.

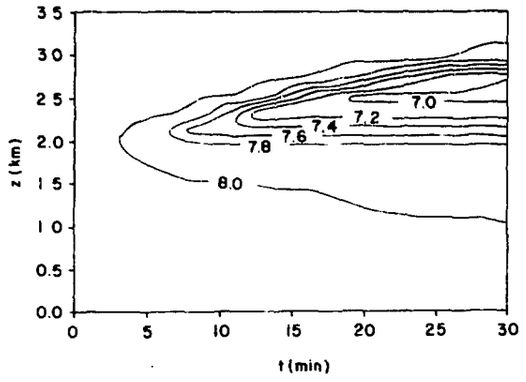

Fig. 1. Temporal and spatial variation of ambient SO_2 concentration (ppb).

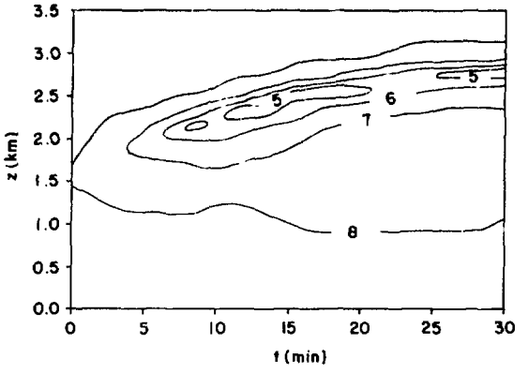

Fig. 2. Temporal and spatial variation of in-cloud SO_2 concentration (ppb).

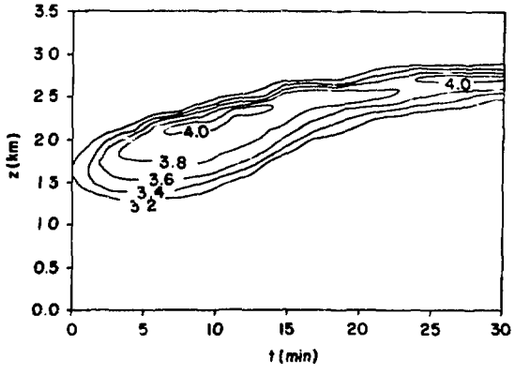

Fig. 3. Temporal and spatial variation of pH in cloud water.

References

Asai, T. and A. Kasahara, 1967: A theoretical study of the compensating downward motions associated with cumulus clouds, J. Atmos. Sci. 24, 487-496.

Davis, W. Jr. and H. J. deBruin, 1964: New activity coefficients of 0-100 percent aqueous nitric acid, J. Inorg. Nucl. Chem. 26, 1069-1083.

Hales, J. M. and D. R. Drewers, 1979: Solubility of ammonia in water at low concentrations, Atmos. Environ. 13, 1133-1148.

Miller, J. M. and R. dePena, 1972: Contribution of scavenged sulfur dioxide to the sulfate of rainwater, J. Geophys. Res. 30, 5905-5916.

Ohta, S., T. Okita, and C. Kato, 1981: A numerical model of acidification of cloud water, J. Meteorol. Soc. Japan 59, 892-901.

Orel A. E. and J. H. Seinfield, 1977: Nitrate formation in atmospheric aerosols, Environ. Sci. Technol. 11, 1000-1007.

RELATIVE CONTRIBUTION TO SULFUR ATMOSPHERIC CONCENTRATIONS AND DEPOSITION FROM LONG-RANGE TRANSPORT

J. D. Shannon

Assessment of the long-range contribution to sulfur deposition is complicated by, first of all, the lack of a common definition of "long-range". If defined on a temporal scale, such as one day's travel from the source, the associated distance can vary widely, depending upon synoptic conditions. If defined on a geopolitical basis, such as the effect of the sources within one state or province upon another state or province, the separation can range from near zero to more than 1000 km.

Typical definitions of long-range transport have lower bounds of 200-500 km. The ASTRAP model (Shannon, 1981) can be modified to include or exclude sources depending on range of source/receptor separation distances. Figures 1 through 5 illustrate pollutant sulfur air concentrations and deposition resulting from sources within 200 km of receptors, sources 200-500 km away, sources 500-1000 km away, and sources beyond 1000 km, respectively, for January and February 1981. Concentrations of SO_2 (Fig. 1) are dominated by sources within 500 km because SO_2 is a primary pollutant that is continuously diminished by transformation and deposition. Dry deposition of SO_2 has similar patterns (Fig. 2). Sulfate, on the other hand, is mainly produced by atmospheric transformation of SO_2 and shows (Fig. 3) significant mid-range and long-range components, as does sulfate dry deposition (Fig. 4). Dry deposition is a continuous process, although at varying rates. Wet deposition, on the other hand, is episodic, and the plume can experience considerable transport before precipitation is encountered. The wet deposition fields (Fig. 5) thus exhibit a relatively greater long-range component than do the dry deposition fields, particularly for the major dry deposited pollutant, SO_2.

Reference

Shannon, J. D., 1981: A model of regional long-term average sulfur atmospheric pollution, surface removal, and net horizontal flux, Atmos. Environ. 15, 689-701.

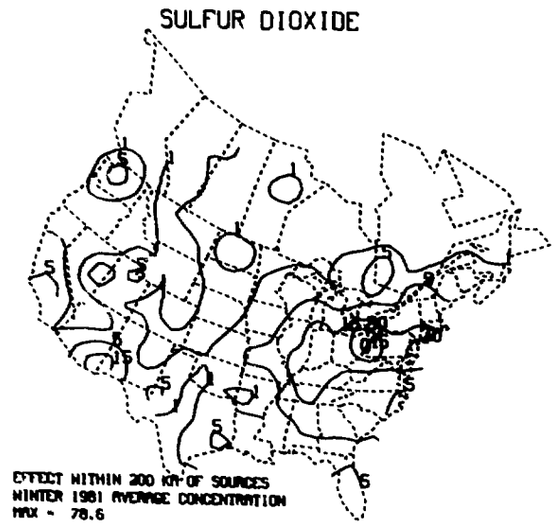

(a)

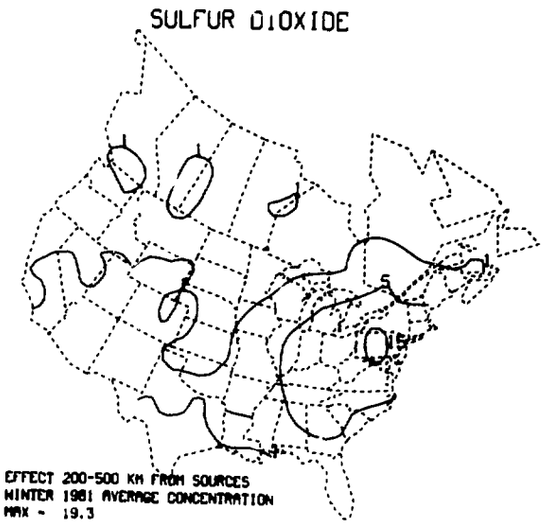

(b)

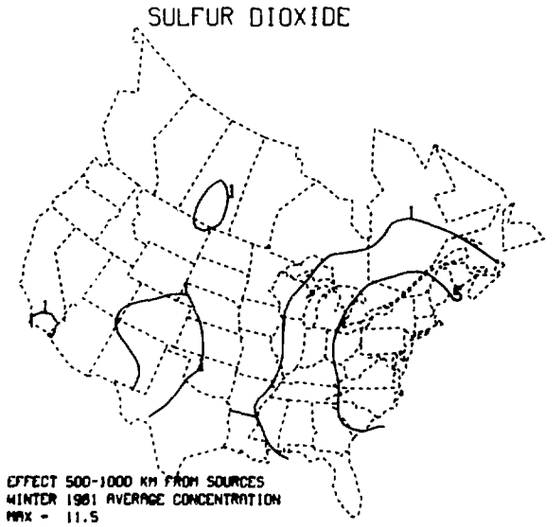

(c)

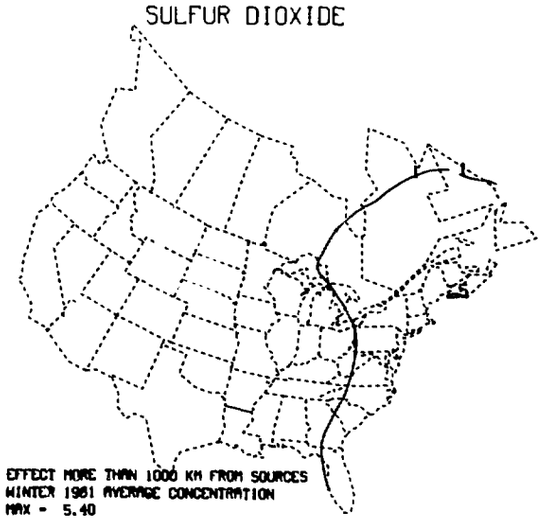

(d)

Fig. 1. Average winter sulfur dioxide concentrations in ($\mu g\ m^{-3}$) resulting from (a) local (<200 km), (b) regional (200 to 500 km), (c) interregional (500 to 1000 km), and (d) distant (> 1000 km) anthropogenic sources.

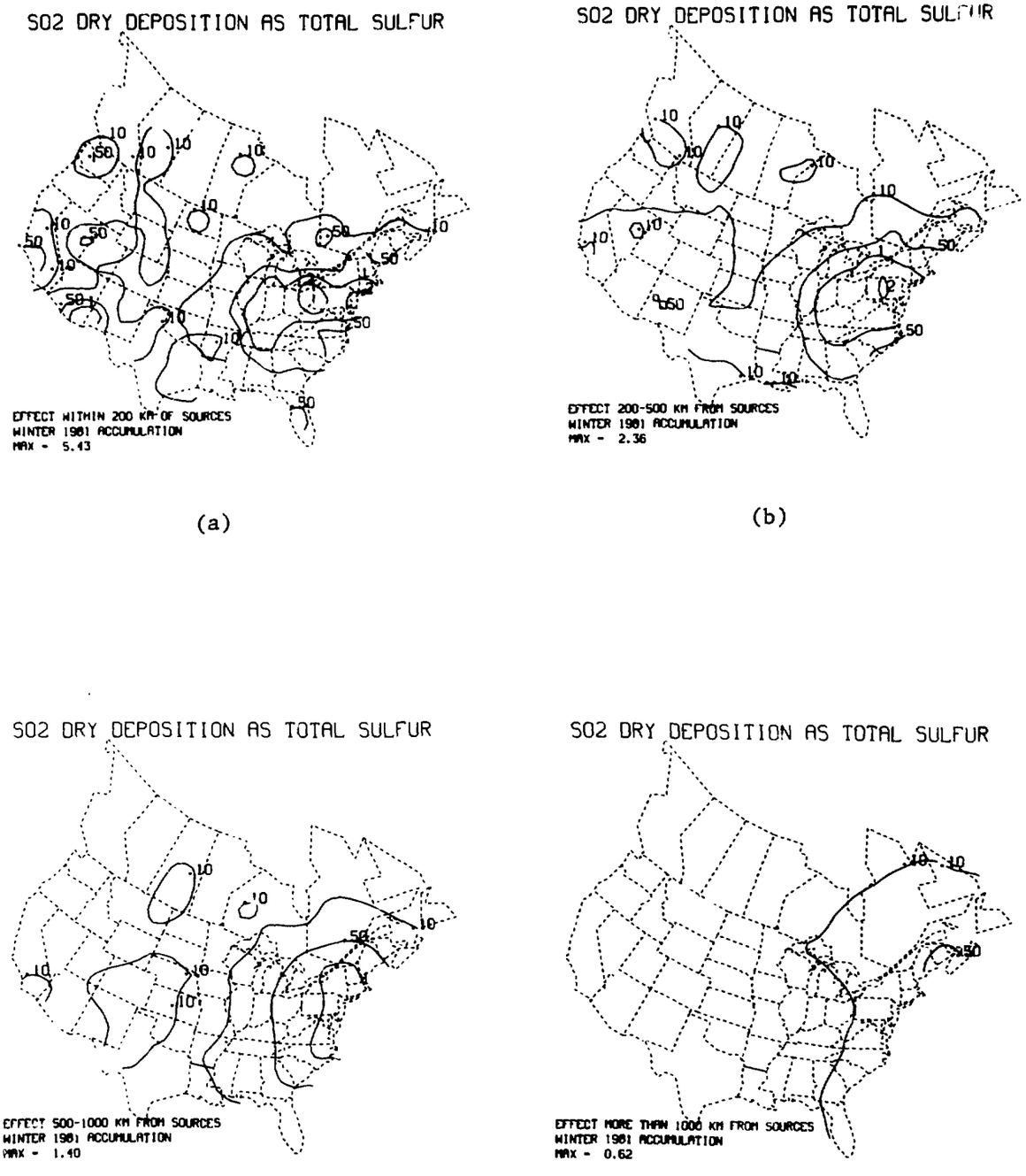

Fig. 2. Cumulative winter sulfur dioxide dry deposition as total sulfur (kg hectare^{-1}) resulting from (a) local (<200 km), (b) regional (200 to 500 km), (c) interregional (500 to 1000 km), and (d) distant (> 1000 km) anthropogenic sources.

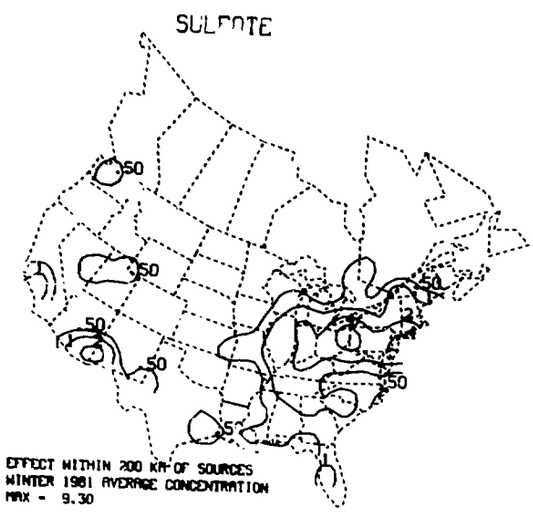

(a)

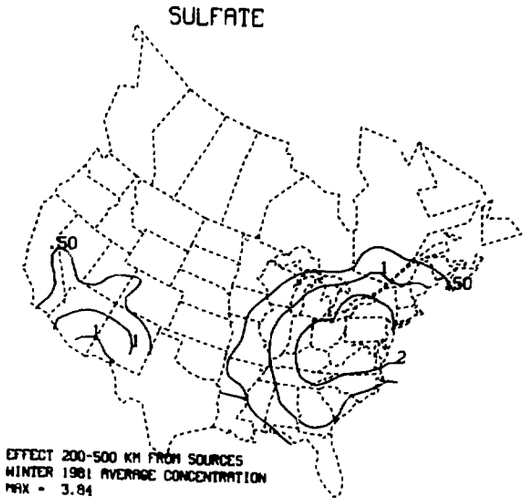

(b)

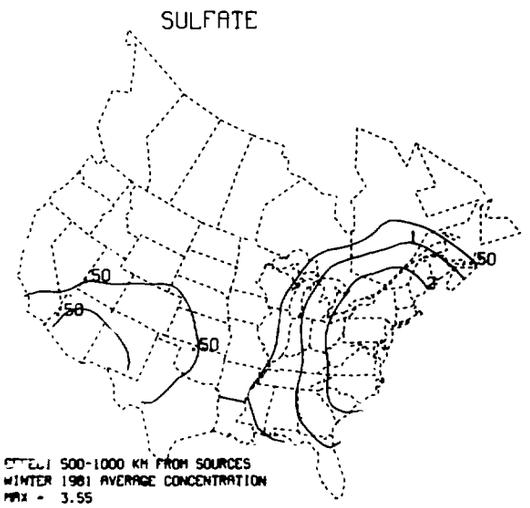

(c)

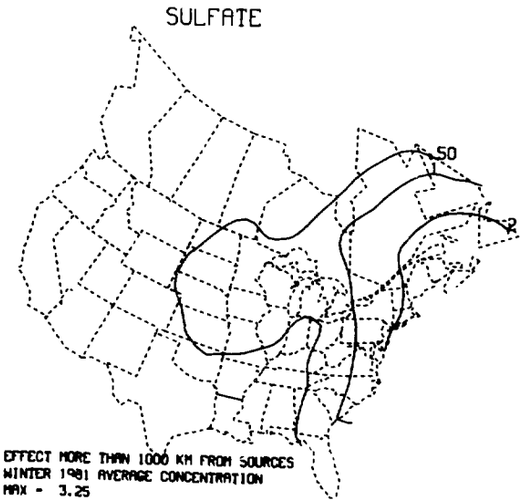

(d)

Fig. 3. Average winter sulfate concentrations (μg m^{-3}) resulting from (a) local (<200 km), (b) regional (200 to 500 km), (c) interregional (500 to 1000 km), and (d) distant (> 1000 km) anthropogenic sources.

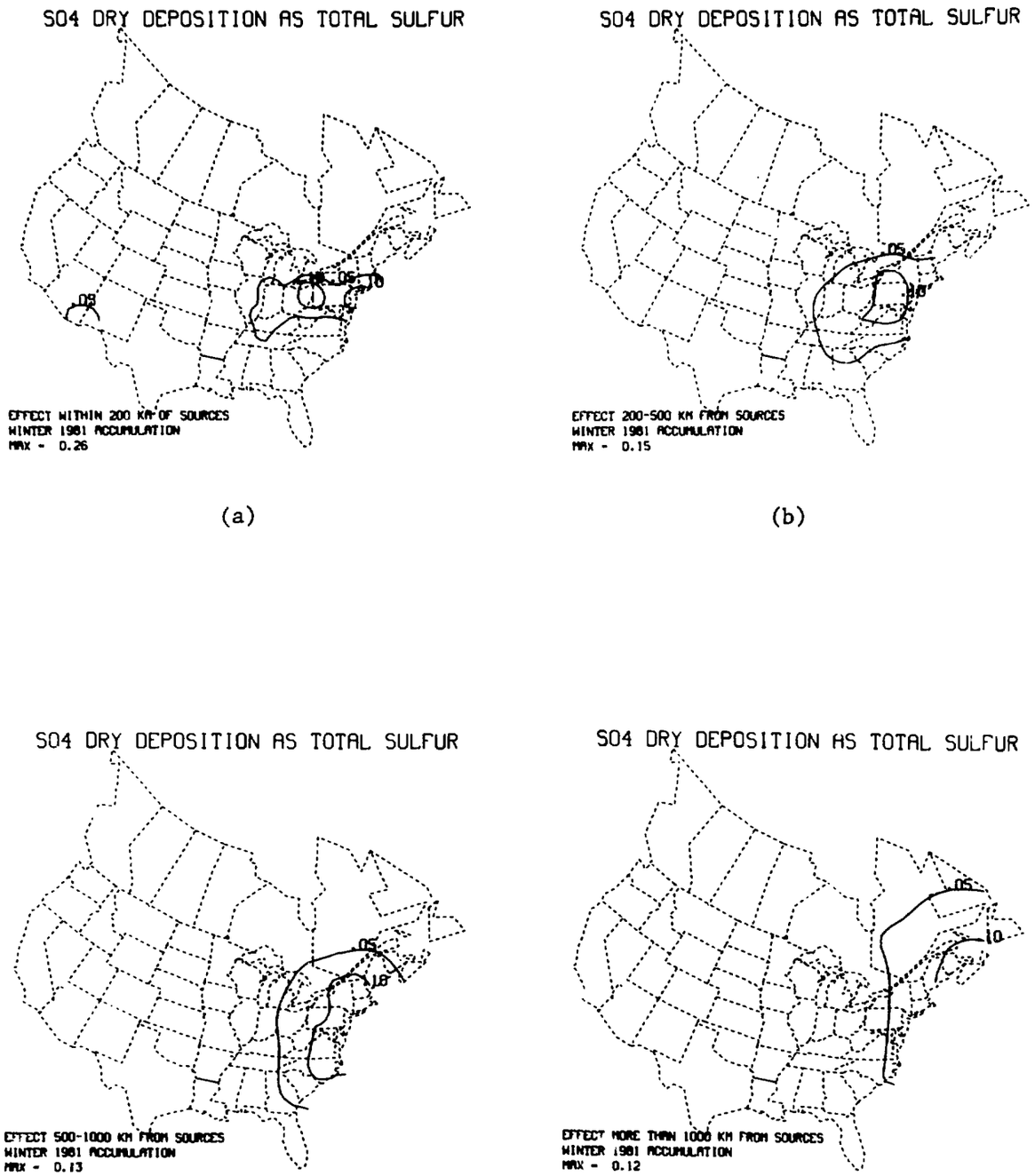

Fig. 4. Cumulative winter sulfate dry deposition as total sulfur (kg hectare^{-1}) resulting from (a) local (<200 km), (b) regional (200 to 500 km), (c) interregional (500 to 1000 km), and (d) distant (> 1000 km) anthropogenic sources.

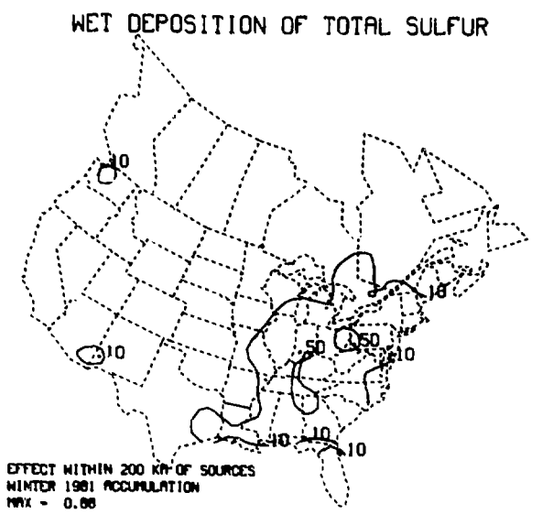

(a)

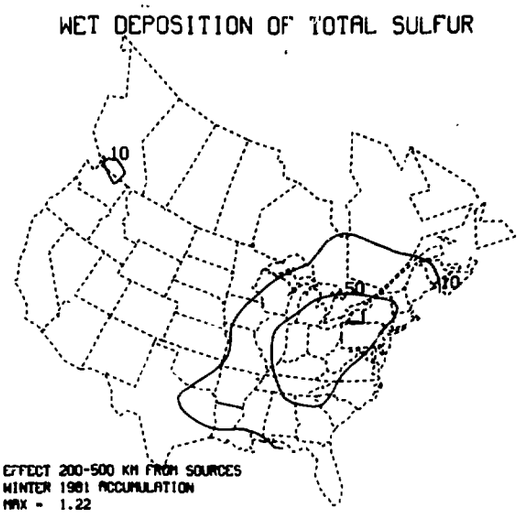

(b)

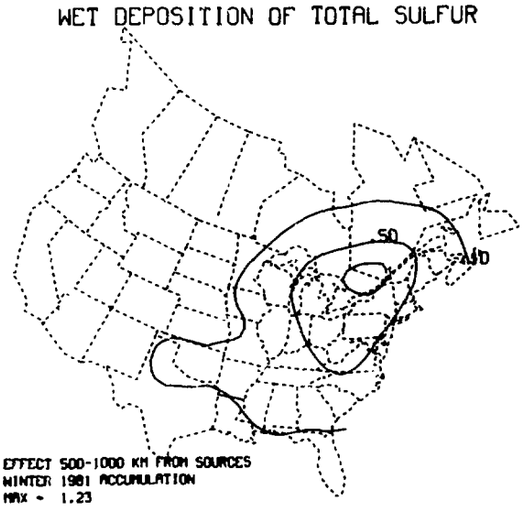

(c)

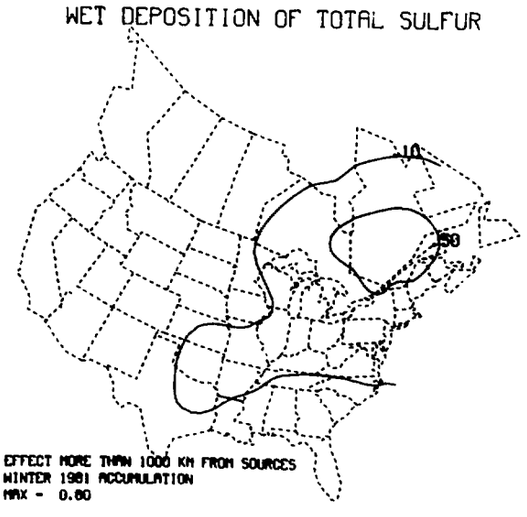

(d)

Fig. 5. Cumulative winter wet deposition of total sulfur (kg hectare^{-1}) resulting from (a) local (<200 km), (b) regional (200 to 500 km), (c) interregional (500 to 1000 km), and (d) distant (> 1000 km) anthropogenic sources.

AN EVALUATION OF WIND FIELD INTERPOLATION SCHEMES USED IN STUDIES OF REGIONAL-SCALE POLLUTANT TRANSPORT

C.-M. Sheih

A study has been conducted to evaluate the numerical schemes most commonly used by modelers for spatial interpolation of wind data from few observation stations. National Weather Service rawinsonde observation stations over the United States (Figure 1) typically are about 450 km apart while numerical models normally require data at about 50 to 100 km intervals. The most common interpolation schemes used in regional-scale simulation to obtain such resolution are:

(A) inverse distance weighting,

(B) inverse distance-squared weighting,

(C) inverse distance-squared and directional weighting (e.g., Heffter, 1980),

(D) using data at the nearest station.

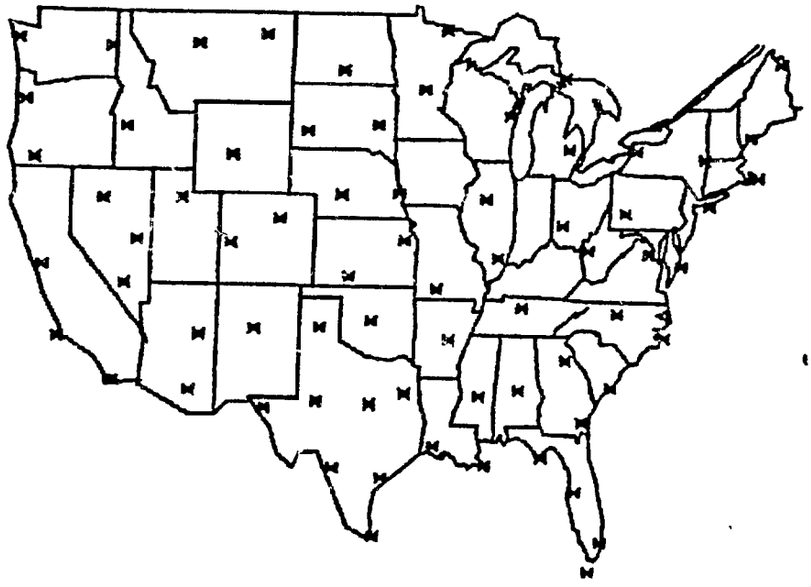

Fig. 1. Location of National Weather Service rawisonde observation stations.

To test these interpolation schemes, we assume that the wind velocity field is a large cyclonic eddy superposed on a uniform wind. The wind velocity components can be expressed by:

$$u = u_a - \omega r \exp(-(r/R)^2) \sin\Theta \quad (1)$$

$$v = v_a + \omega r \exp(-(r/R)^2) \cos\Theta \ , \quad (2)$$

where u and v are easterly and northerly total wind velocity components, u_a and v_a are the uniform velocity components, ω is the angular velocity of the cyclone, r and θ are the radial and angular coordinates of the polar coordinate system with reference to the center of the cyclone for radial distance and to the east for the azimuth angle, and R is a length scale characterizing the size of the cyclone.

For the present study, the parameters are set at $u_a = v_a = 5$ m s^{-1}, $\omega = 2.8\ u_a R^{-1}$, R = 800 km, and the cyclone is located near the center of the United States. The theoretical values of the wind velocity components at the observation stations in Figure 1 are computed from Eqs. (1) and (2). These values are then used in the four numerical schemes to obtain the interpolated values at the grid points of an 80-km grid mesh covering the entire United States. These results are compared with the theoretical values computed from Eqs. (1) and (2) for these grid points. The standard deviation errors of wind speed, wind direction, and divergence ($\partial u/\partial x + \partial v/\partial y$) for the entire grid network is shown in Table 1, where x and y are positive eastward and northward, respectively. For this test the best scheme is B, followed by A, C, and D.

To test the effect upon trajectory calculations, we assume that a simulated particle is released at a distance 0.25R west of the cyclone center. The coordinates of the theoretical trajectory are obtained by using $\Theta = \omega t$ and integrating Eqs. (1) and (2) with respect to time t, which yields:

$$x_p(t) = x_p(0) + u_a t - r_p \exp(-(r_p/R)^2 (\cos\omega t - 1) \quad (3)$$

$$y_p(t) = y_p(0) + v_a t + r_p \exp(-(r_p/R)^2) \sin\omega t \ , \quad (4)$$

Table 1. Comprison of various interpolation schemes

Interpolation scheme	Standard deviation errors with respect to theoretical values: Wind speed % of speed maximum	Rank	Direction degree	Rank	Divergence s^{-1}	Rank	Cumulated Rank
(A) Inverse distance	3.6	2	16.4	2	2.1×10^{-6}	1	5
(B) Inverse distance-squared	3.3	1	14.9	1	2.1×10^{-6}	1	3
(C) Inverse distance-squared and directional weighting	18.8	3	32.1	3	6.5×10^{-6}	2	8
(D) Nearest station	22.3	4	38.1	4	1.3×10^{-5}	3	11

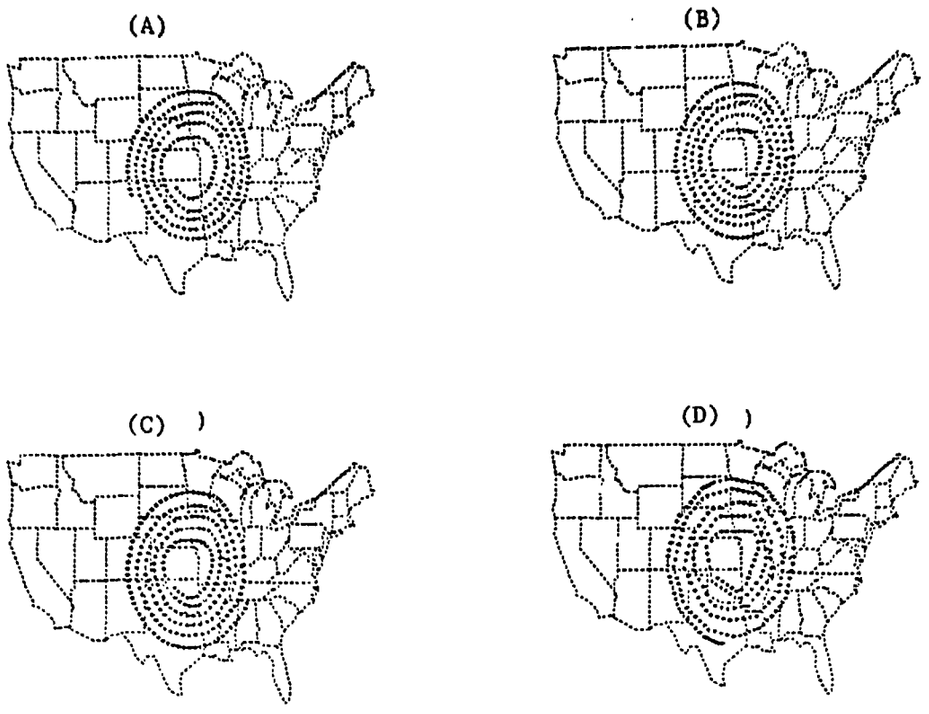

Fig. 2. Trajectories computed from interpolation schemes A, B, C, and D for a stationary cyclone.

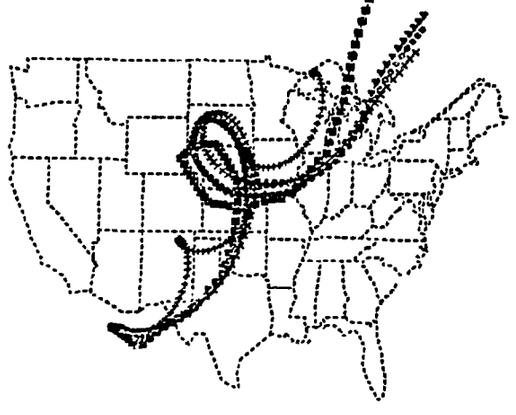

Fig. 3. Trajectories for theoretical solution (+) and the interpolation schemes A(x), B(◇), C(△), and D(□) for a cyclone moving from southwest to northeast.

where p indicates particle and r_p = 0.25 R. The simulated trajectories ar computed with the velocity fields produced by the four interpolation schemes with the time increment set to $0.5(\Delta x/U_{max})$ to maintain consistency wit numerical requirements, where Δx = 80 km is the grid mesh length and U_{max} i the theoretical maximum wind speed of the entire field. The simulate trajectories with $u_a = v_a = 0$ are shown in Figure 2. All the trajectories ar terminated at the same time after release. The theoretical trajectory (no shown here) is simply a closed circle. Thus, the smaller the radius of th trajectory of an interpolation scheme the better it approximates th theoretical one. As indicated in Figure 2, for this criterion the rank o interpolation schemes in trajectory accuracy is A, B, C, and D. The rankin of the schemes, however, depends upon wind-field conditions and the locatio of particle release. For example, the results of a more realistic wind-flo pattern with $u_a = v_a = 5$ m s^{-1} and with a particle released at 0.25R west o the center of a cyclone located near the border of Texas and Mexico are show in Figure 3. The theoretical trajectory exhibits three small loops, whil only one large loop appears for each of the interpolation schemes. Althoug none of the schemes gives a satisfactory prediction of the trajectory interpolation scheme D seems to give the poorest prediction in the loopin region but becomes the best predictor at the end of the trajectory Interpolation scheme C, which includes directional weighting, would b expected to give best relative results in a wind field containing wind spee "jets", but the definition and analytical solution of such wind fields considerably more difficult.

Reference

Heffter, J. L., 1980: Atmospheric transport and dispersion model, National Oceanic and Atmospheric Administration Technical Memorandum. Memo. E ARL-81, 24 pp.

SIMULATIONS OF MESOSCALE MOTIONS OVER LAKE MICHIGAN WITH A PLANETARY BOUNDARY LAYER MODEL

I.-Y. Lee

Numerical simulations have been conducted to investigate the effects of Lake Michigan on mesoscale motions. A two-layer planetary boundary layer (PBL) model (Lee and Swan, 1977) has been expanded to include three layers: the conventional PBL, a convective layer on top of the PBL, and the free atmosphere above. The dynamic parameters within the convective layer and the free atmosphere are computed according to synoptic conditions. The depth of the PBL and the average values of the fields within it are determined by numerically integrating the pertinent vertically averaged conservation equations. The horizontal distribution of the convective layer wind, temperature, and moisture content, plus associated vertical gradients, are required for boundary conditions at the top of the PBL, and the surface topography and physical parameters of the surface are necessary for lower boundary conditions. The fluxes of variables at the surface and at the interface are calculated using parameterizations such as given by Deardorff (1972), and a prognostic equation for surface temperature variation is solved that takes into account solar and terrestial radiation, sensible heat flux, and latent heat flux of evaporation.

A test was carried out for the gridded target area as shown in Figure 1, with a topographic resolution of 1/3 degree. Initial and boundary values were determined from soundings at Green Bay, Wisconsin; Peoria and Salem, Illinois; Dayton, Ohio; and Flint, Michigan. The soundings on July 1, 1978, indicated that the prevailing wind was southeasterly in the PBL and northwesterly in the free atmosphere throughout the day, and that the moisture convergence occurred over the northern and eastern part of the target area during the afternoon. The fields of simulated PBL wind, PBL depth, and PBL-surface potential temperature difference at 1800 CST on July 1, 1978, are presented in Figures 2, 3 and 4, respectively. These fields were obtained after 12 hours of real time simulation.

The effects of the lake on the behavior of the PBL motions are evident. The prevailing southeasterly wind in the PBL evolves during the daytime to

exhibit some interesting mesoscale patterns in the simulated field. These patterns result from the differential surface heating over land and water. Light winds are from near the southern and eastern shores of the lake as a result of lake breeze working against the southeasterly wind. On the other hand, strong winds are observed near the western shore as the prevailing southeasterly wind is augmented by the lake breeze induced by strong convective instability occurring during the daytime over land. In terms of the potential temperature difference between the surface and the bulk PBL, the field of vertical sensible heat transfer shows a cold tongue extending north to south along the western coastline of the Lake Michigan. The horizontal gradient of the sensible heat is greater over the eastern regions of the trough line than over the western regions. This pattern of temperature difference is clearly reflected in the field of PBL depth, since the associated sensible heat flux modulates convective instability. As warm air enters the PBL from the eastern and southern boundary, the strong mixing caused by convective instability deepens the PBL. On the other hand, the cooling by the lake breeze seems to be important in producing a more shallow boundary layer near the western side of Lake Michigan.

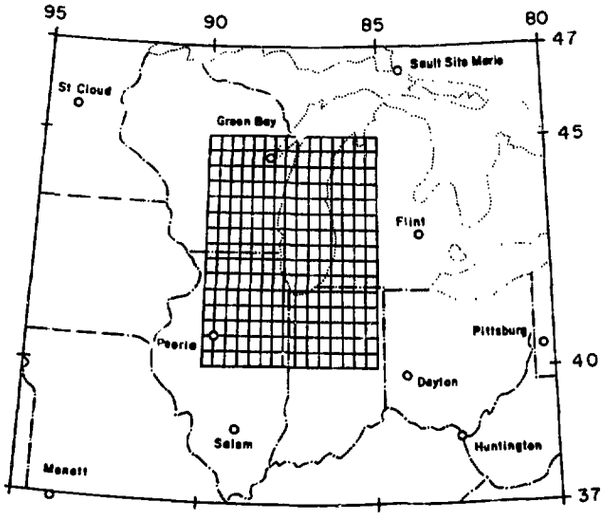

Fig. 1. Map of the Lake Michigan area showing locations of sounding stations. Data for the present simulation was obtained from the five stations within and nearest the target gridded area.

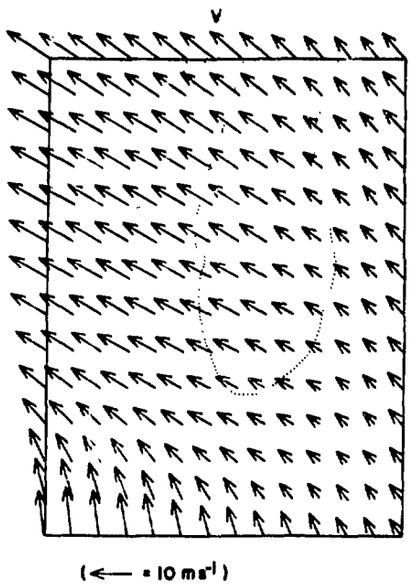

Fig. 2. The PBL wind field computed for 1800 CST, 1 July 1978.

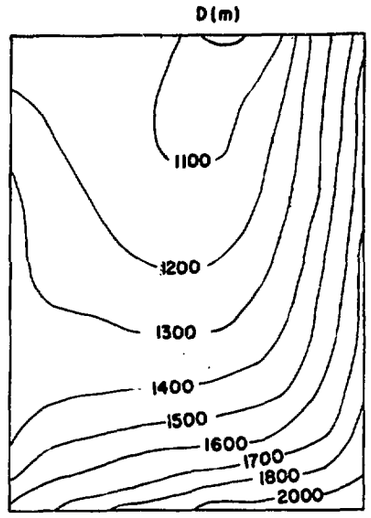

Fig. 3. Computed field of PBL depth D above ground level at 1800 CST, 1 July 1978.

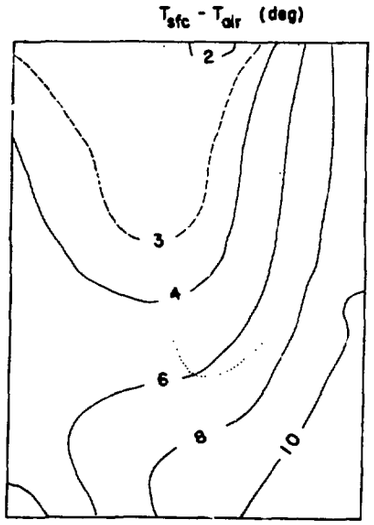

Fig. 4. Computed field of potentional temperature deviation between the bulk PBL and surface at 1800 CST, 1 July 1978.

References

Deardorff, J. W., 1972: Parameterization of the planetary boundary layer for use in general circulation models, Mon. Wea. Rev. 100, 93-106.

Lee, I.-Y. and P. R. Swan, 1977: Transport of contaminants in the planetary boundary layer, Preprints, Joint Conference on Applications of Air Pollution Meteorology, American Meteorological Society, Boston, MA 392-399.

EFFECTS OF SURFACE WETNESS ON THE BEHAVIOR OF AIRBORNE PARTICLES

I.-Y. Lee and M. L. Wesely

Observations of vertical particle fluxes measured by eddy correlation at a height of 8 m over Lake Michigan (Wesely and Williams, 1981) and at heights of 5-6 m over wet surfaces (Wesely and Hicks, 1979) show somewhat enigmatic features. Over Lake Michigan, particle fluxes measured by a sensor called the "charger" that detects particles smaller than about 0.05 μm in radius are directed upward, away from the surface, and fluxes measured by a nephelometer that detects particles greater than about 0.2 μm in radius are directed downward, toward the surface. The charger fluxes are directed upward in the high relative humidities found in the morning over some land surfaces and over snow, but are directed downward over many drier surfaces. These features are somewhat unexpected in light of other field experimental information, such as that provided by Davidson and Frieldlander (1978) on submicron particles or by Wesely et al. (1983) on submicron sulfur. One question is whether these fluxes are representative of fluxes much closer to the surface or if there is a significant change of flux with height.

Preliminary computations have been carried out to simulate the spectral evolution of fine particles near wet surfaces with an aerosol numerical model (Lee, 1983) that describes homogeneous gas kinetics, nucleation, and growth by heteromolecular diffusion and coagulation. To simplify the situation, we have assumed that a steady-state and stratified atmosphere surface layer exists with respect to the moisture contents. The nature of this condition is such that the air is saturated within the quasilaminar sublayer, and thereafter the relative humidity undergoes a logarithmic decrease with height. Initially, all the gaseous and particulate species were assumed to have concentrations appropriate for a clean continental background. The assumption of steady state undoubtedly overemphasizes the change of particle characteristics with height because in many cases the vertical mixing that usually occurs in the atmospheric surface layer is too rapid to allow particles to be in total equilibrium with local ambient conditions.

The calculated equilibrium vapor pressures for free sulfuric acid molecules (P_{env}) and for sulfuric acid (P_{drop}) found in particles of 0.01 μm in

radius are shown in Figure 1 for various relative humidities. The pressure drop between P_{env} and P_{drop} clearly increases with increasing relative humidity, largely because more small particles are produced with greater relative humidity. The slow increase of P_{env} at low relative humidity is considerably less than the sharp increase of P_{drop} at corresponding relative humidities. This increase of P_{drop} is mainly due to the increase of weight, by percentage, of H_2SO_4 in droplets at low relative humidity. On the other hand, the increase of P_{drop} with decreasing relative humidity is insignificant for large particles (not shown here, but the variation of P_{drop} with relative humidity is nearly zero). Therefore, for this size range, the slow increase of P_{env} seems to affect the spectral evolution such that more nephelometer particles are produced at low relative humidity.

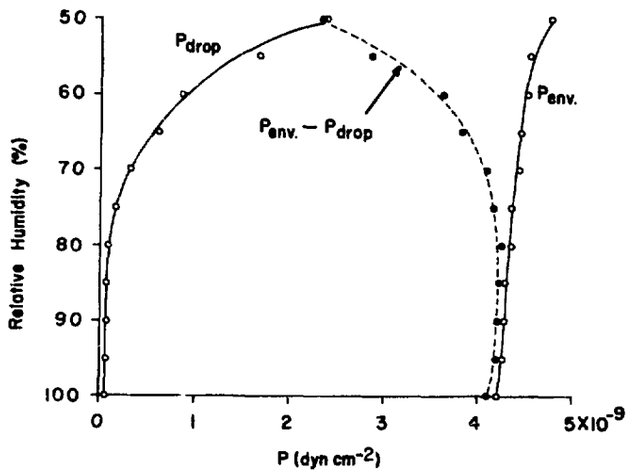

Fig. 1. Profiles of partial pressure of sulfuric acid vapor in the environment P_{env}, at the droplet surface P_{drop}, and the deviation $P_{env}-P_{drop}$.

The temporal evolution and the steady state profiles of charger and nephelometer particle concentrations are presented in Figures 2 and 3, respectively. As expected, more charger particles are produced at high relative humidity and conversely for nephelometer particles. The steady state concentration profiles indicate clearly that the phenomena of psuedofluxes may occur over wet surfaces, namely, upward fluxes of charger particles and downward fluxes of nephelometer particles, if the eddy fluxes are directed in accordance with normal flux/gradient relationships. However, the question of whether these gradients caused by humidity gradients can persist in a turbulent field such as normally found in the atmospheric surface layer remains unanswered at present.

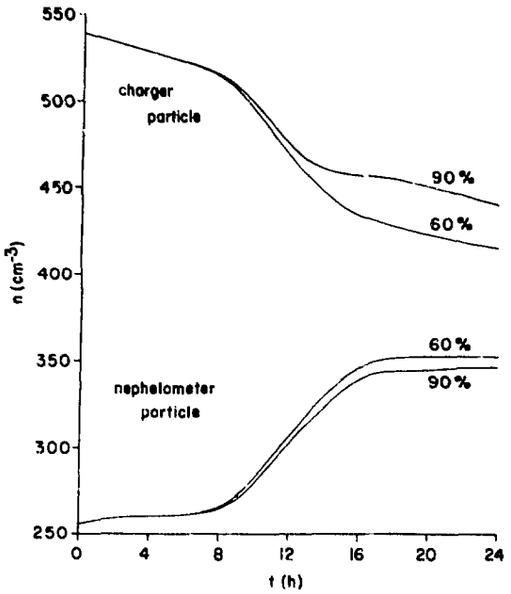

Fig. 2. Evolution of charger and nephelometer particles at relative humidities of 60% and 95%.

Fig. 3. Steady state profile of charger and nephelometer particle concentrations with varying relative humidity under the assumption of zero fluxes at the surface.

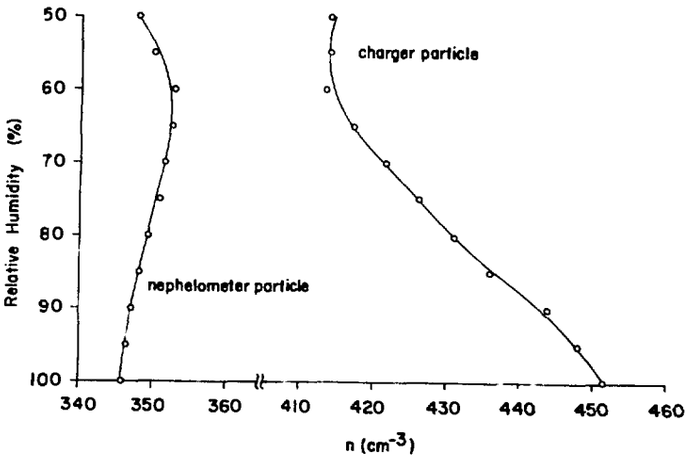

References

Davidson, C. I. and S. K. Friedlander, 1978: A filtration model for aerosol dry deposition: Application to trace metal deposition from the atmosphere, J. Geophys. Res. 83, 2343-2352.

Lee, I. Y., 1983: Formations of sulfate in cloud-free environment, J. Appl. Meteorol. 22, 163-170.

Wesely, M. L. and B. B. B. Hicks, 1979: Dry deposition and emission of small particles at the surface of the earth, Preprint Volume, Fourth Symposium of Turbulence, Diffusion, and Air Pollution, Reno, NV, January 15-18, 1980, American Meteorological Society, Boston, pp. 510-513.

Wesely, M. L. and R. M. Williams, 1981: Eddy-correlation measurements of particle fluxes over Lake Michigan, Argonne National Laboratory Radiological and Environmental Research Division Annual Report, ANL-80-115, Part IV, Argonne National Laboratory, Argonne, IL, pp. 36-38.

Wesely, M. L., D. R. Cook, R. L. Hart, B. B. Hicks, J. L. Durham, R. E. Speer, D. H. Stedman, and R. J. Tropp, 1983: Eddy-correlation measurements of dry deposition of particulate sulfur and submicron particles, Precipitation Scavenging, Dry Deposition, and Resuspension, Vol. 2, H. R. Pruppacher, R. G. Semonin, and W. G. N. Slinn, Eds., Elsevier, New York, pp. 943-952.

ON THE TRANSPORT OF GASES AND PARTICLES THROUGH POORLY MIXED INTERFACIAL SUBLAYERS

M. L. Wesely

Direct measurements in the field of the vertical exchange rates of gases other than water vapor above water surfaces are very few. Some of the most well known data are from the radon evasion experiments (e.g., Peng et al., 1979). Although there is a considerable amount of scatter in those data, they roughly agree with predictions based on surface renewal theory for the aqueous interfacial sublayer in which the Schmidt number has an exponential value of 0.5 and empirical constants are derived from heat transfer measurements (Wesely et al., 1982). A great deal of theoretical and laboratory research has been conducted on the rate of gas transfer through the uppermost skin of water in oceans and lakes, but the importance of transfer aided by bubbles has only recently been systematically studied in wind-water tunnels (e.g., Merlivat and Memery, 1983). It is possible that a transfer mechanism associated with bubbles partially short-circuits the rather high resistance to vertical transport of nonreactive gases through the water skin, so that a traditional Schmidt-number scaling might not always be appropriate. Clearly, better explanations are needed to account for the very large values of CO_2 transfer above ocean in moderate wind speeds (Wesely et al., 1982).

The transfer of submicron particulate sulfate to the surface of the earth is often assumed to be quite small, and the theoretical arguments for this case are based on the effects of a very small molecular (Brownian) diffusivity in limiting transfer of submicron particles through the quasilaminar layer of air enveloping surface elements. As in the case of gas transfer through poorly mixed interfacial water sublayers, however, any means by which the high resistance of the sublayer could be short circuited would serve the purpose of substantially increasing the transport to the surface. For example, there seems to be some process that accomplishes this enchanced transport of airborne submicron particulate sulfur to aerodynamically rough surfaces (Wesely et al., 1983). The transfer velocity at moderate wind speeds in atmospherically unstable conditions seems to be enhanced by more than an order of magnitude, but the extent of enhancement in near-neutral and stable atmospheric

conditions is usually much smaller. The fact that the extent of this increase of transfer velocity for unstable conditions is near that associated with CO_2 evasion from the ocean in moderate wind speeds might be fortuituous because the mechanisms increasing the transfer could be much different in the two situations.

References

Merlivat, L. and L. Memery, 1983: Gas exchange across an air-water interface: Experimental results and modeling of bubble contribution to transfer, J. Geophys. Res. 88, 707-724.

Peng, T.-H., W. S. Broecker, G. G. Mathieu, Y.-H. Li, and A. E. Bainbridge, 1979: Radon evasion rates in the Atlantic and Pacific Oceans determined during the GEOSECS program, J. Geophys. Res. 84, 2471-2486.

Wesely, M. L., D. R. Cook, R. L. Hart, and R. M. Williams, 1982: Air-sea exchange of CO_2 and evidence for enhanced upward fluxes, J. Geophys. Res. 87, 8827-8832.

Wesely, M. L., D. R. Cook, R. L. Hart, B. B. Hicks, J. L. Durham, R. E. Speer, D. H. Stedman, and R. J. Tropp, 1983: Eddy-correlation measurements of the dry deposition of particulate sulfur and submicron particles, Precipitation Scavenging, Dry Deposition and Resuspension, Vol. 2, H. R. Pruppacher, R. G. Semonin, and W. G. N. Slinn, Eds., Elsevier, New York, pp. 943-952.

PARAMETERIZATIONS OF EVAPOTRANSPIRATION AND SENSIBLE HEAT FLUX FROM FIELD GRASS

D. R. Cook

A simple model that parameterizes evapotranspiration was tested and reported previously (Cook, 1981). The same model is used here with data from the June 1982 Dry Deposition Intercomparison Experiment near Champaign, Illinois, to develop parameterizations of both evapotranspiration and sensible heat flux. The equilibrium model of Priestley and Taylor (1972) takes the form:

$$LE = \alpha'\left(\frac{s}{s+\gamma}\right)(Rn-G) \quad , \tag{1}$$

or as modified by Barton (1979),

$$LE = \frac{\alpha\sigma s}{\sigma s+\gamma}\,(Rn-G) \quad , \tag{2}$$

where LE is actual evapotranspiration, s is the slope of the saturation vapor pressure-temperature curve, γ is the psychrometric coefficient, Rn is the net radiation, G is the surface soil heat flux, α' is the ratio of actual to equilibrium evapotranspiration, α is a quantity that is dependent upon surface type, and σ is a measure of surface moisture availability. The quantity α' varies with both surface type and surface moisture availability. The radiation energy budget (in W m^{-2}) and soil moisture (in % water by volume) were measured and averaged to give the daily budget for the period of positive evapotranspiration. Meteorological conditions on 7 of 13 days were suitable for anlaysis.

Since Eq. (2) has certain computational advantages over Eq. (1), it has been used for the present parameterizations. The term σ is derived as a function of soil moisture (sm):

$$\sigma = \frac{1.10\ sm}{0.28 + sm} \quad , \tag{3}$$

with all other quantities in Eq. (2) being determined as previously outlined by Cook (1981). Since it is desirable to apply the parameterization of

Eq. (2) with a minimum of measured quantities in order to predict LE and sensible heat flux (H), only Rn, sm and σ are needed. The quantity s is easily computed from the air temperature (T) at a few meters and Eq. (4), which was derived from Eq. (8) in Buck (1981):

$$s = 6.14 \exp\left(\frac{17.502T}{240.97 + T}\right)\left(\frac{4217.46T}{(240.97 + T^2)}\right), \qquad (4)$$

for atmospheric station pressure near 1000 mb. The term γ is 0.67 $\pm$ 0.01, while a good estimate of G is 0.25 x Rn. The quantity α computed from the present data would seem to indicate that far less than potential evapotranspiration conditions prevailed, even though soil moistures were sufficient at all times to support potential evapotranspiration. The smaller than expected measurements of LE during the experiment seen to indicate that evapotranspiration was being hindered or suppressed by some factor. Heavy matting, near the soil surface, of grass mowed a month before the experiment and the apparently quasi-senescent state of the grass during the experiment may have resulted in a condition of less than free transpiration. This is suggested by the relative insensitivity of the model to a wide range of soil moisture. Therefore, it is suggested that atypical conditions existed during the experiment, resulting in an α value less than would likely occur had the grass been left to grow naturally, unmowed. The parameterizations below may, as a result, be atypical.

De Bruin and Holtslag (1979) suggest that Eq. (2) underestimates LE by a constant factor. For the present data this is unfortunately too simple an approach. It is not intuitively or physically obvious that Eq. (2) needs be an underestimate, even under potential conditions. In fact, for the present data, Eq. (2) is generally an overestimate for 89 W m^{-2} < LE <123 W m^{-2} and an underestimate otherwise, resulting in the expression below, derived from the equation for an axis-shifted hyperbola:

$$LEM = \frac{-10942.48 + 84.48\ LEC}{LEC - 127.52}, \qquad (5)$$

where LEC is the evapotranspiration calculated with Eq. (2) and LEM is the measured evapotranspiration. Equations (2) and (5), when combined, provide a model that adequately predicts LE for the conditions of the experiment.

Sensible heat flux can be predicted as well by finding the calculated value HC as the residual of the energy budget,

$$HC = Rn - G - LEC \ , \tag{6}$$

and then applying a linear regression that describes the measured sensible heat flux (HM) as a function of HC,

$$HM = 0.80HC + 33.95 \ . \tag{7}$$

Because of the limited amount of data presented, it is necessary for more measurements to be made before the model can be realiably used. Even so, the specificity of surface conditions in this study precludes general use of the model results.

References

Barton, I. J., 1979: A parameterization of the evaporation from nonsaturated surfaces, J. Appl. Meteorol. 18, 43-47.

Buck, A. L., 1981: New equations for computing vapor pressure and enhancement factor, J. Appl. Meteorol. 20, 1527-1532.

Cook, D. R., 1981: Effects of soil moisture on evapotranspiration from fescue grass, Argonne National Laboratory Radiological and Environmental Research Division Annual Report, ANL-81-85, Part IV, pp. 21-26.

De Bruin, H. A. R. and A. A. M. Holtslag, 1982: A simple parameterization of the surface fluxes of sensible and latent heat during daytime compared with the Penman-Monteith Concept, J. Appl. Meteorol. 21, 1610-1621.

Priestley, C. H. B. and R. J. Taylor, 1972: On the assessment of surface heat flux and evaporation using large-scale parameters, Mon. Wea. Rev. 100, 81-92.

PUBLICATIONS BY THE STAFF OF THE ATMOSPHERIC PHYSICS SECTION FOR THE PERIOD JANUARY-DECEMBER 1982

Journal Articles and Book Chapters

J. D. Shannon and E. C. Voldner
ESTIMATION OF CONCENTRATION AND DEPOSITION OF POLLUTANT SULFUR IN EASTERN CANADA AS A FUNCTION OF MAJOR SOURCE REGIONS
Water, Air and Soil Pollut. 18, 101-104.

D. L. Sisterson and P. M. Irving
TROUBLESHOOTING pH AND CONDUCTIVITY MEASUREMENTS, APPENDIX 2, DIAGNOSTIC CHAPTER ON pH AND CONDUCTIVITY MEASUREMENTS FOR THE NATIONAL ATMOSPHERIC DEPOSITION PROGRAM FIELD OBSERVER INSTRUCTION MANUAL
NADP Instruction Manual-site operation. Prepared by D. S. Bigelow, National Atmospheric Deposition Program, Natural Resource Ecology Laboratory, Colorado State University, Fort Collins, CO 80523.

D. R. Shin and I. Y. Lee
NUMERICAL STUDIES TO DETERMINE SITES OF WIND ENERGY CONVERSION SYSTEM
J. Solar Energy Society of Korea 2, 33-34.

A. J. Dyer and B. B. Hicks
KOLMOGOROFF CONSTANTS AT THE 1976 ITCE
Boundary-Layer Meteorol. 22, 135-150

B. B. Hicks, M. L. Wesely, and J. D. Durham
CRITIQUE OF METHODS TO MEASURE DRY DEPOSITION, CONCISE SUMMARY OF WORKSHOP
Energy and Environmental Chemistry, Vol. 2., (ed. L. H. Keith), Ann Arbor Publishers, pp. 205-223.

M. L. Wesely
SIMPLIFIED TECHNIQUES TO STUDY COMPONENTS OF SOLAR RADIATION
J. Appl. Meteorol. 21, 373-383.

M. L. Wesely, J. A. Eastman, D. H. Stedman, and E. D. Yalvac
AN EDDY-CORRELATION MEASUREMENT OF NO_2 FLUX TO VEGETATION AND COMPARISON TO O_3 FLUX
Atmos. Environ. 16, 815-820.

D. R. Cook and J. M. Norman
SOIL WARMING AS AN ALTERNATIVE TO CONVENTIONAL WASTE-HEAT DISSIPATION
J. Environ. Qual. 11, 45-52.

M. L. Wesely, D. R. Cook, R. L. Hart, and R. M. Williams
AIR-SEA EXCHANGE OF CO_2 AND EVIDENCE FOR ENHANCED UPWARD FLUXES
J. Geophys. Res. 27, 8827-8832.

A. J. Dyer, J. R. Garratt, R. J. Francey, I. C. McIlroy, N. E. Bacon, P. Hyson, E. F. Bradley, O. T. Denmead, L. R. Tsvang, Y. A. Volkov, B. M. Kprov, L. G. Elagina, K. Sahashi, N. Monji, T. Hanafusa, O. Tsukamoto, P. Frenzen, B. B. Hicks, M. L. Wesely, M. Miyake, and W. Shaw
AN INTERNATIONAL TURBULENCE COMPARISON EXPERIMENT (ITCE 1976)
Boundary-Layer Meteorol. 24, 181-209.

B. B. Hicks, M. L. Wesely, J. L. Durham, and M. A. Brown
SOME DIRECT MEASUREMENTS OF ATMOSPHERIC SULFUR FLUXES OVER A PINE PLANTATION
Atmos. Environ. 16, 2899-2903.

Conference Proceedings and Miscellaneous Reports

J. D. Shannon, L. Kleinman, C. Benkovitz, and C. Berkowitz
INTERCOMPARISON OF MAP3S MODELS OF LONG-RANGE TRANSPORT AND DEPOSITION
Proceedings of the Third Joint Conference on Applications of Air Pollution Meteorology, San Antonio, TX, AMS, pp. 29-32, 11-15 January 1982.

J. D. Shannon
LONG-RANGE TRANSPORT MODELING (CHAPTER 3.2) FINAL NORTHEAST REGIONAL ENVIRONMENTAL IMPACT STATEMENT, THE POTENTIAL CONVERSION OF FORTY-TWO POWERPLANTS FROM OIL TO COAL OR ALTERNATE FUELS.
DOE/EIS-0083-F, 3-16 to 3-29 (1982).

R. L. Coulter
CIRCULATION CHARACTERISTICS DURING ASCOT 1980
Proceedings of the 2nd Conference on Mountain Meteorology, Steamboat Springs, CO, AMS, 7.11, pp. 316-320, 9-12, November 1981.

W. Porch, W. R. Fritz, R. P. Hosker, and R. L. Coulter
COMPARISON OF CROSS-PATH OPTICAL ANEMOMETER DATA FROM ASCOT 1979 AND 1980 EXPERIMENTS
UCID-19358, ASCOT-82-1, 37 pp.

Distribution for ANL-82-65 Part IV

Internal:

W. E. Massey
H. Drucker
E. G. Pewitt
K. L. Brubaker
D. R. Cook
R. L. Coulter
E. J. Croke
J. D. DePue
A. J. Dvorak
P. Failla
P. Frenzen
P. F. Gustafson
R. L. Hart
P. E. Hess
B. D. Holt
E. Huberman
M. Inokuti
S. A. Johnson
R. Kumar
I-Y. Lee
B. M. Lesht
T. J. Martin
J. E. Miller
D. P. O'Neil
A. J. Policastro
J. J. Roberts
D. M. Rote
S. J. Rudnick
J. D. Shannon
C. M. Sheih
D. L. Sisterson
R. W. Springer
C. M. Stevens
D. G. Streets
P. Tyrolt (5)
M. L. Wesely
G. A. Zerbe
APP/ER Library (100)
A. B. Krisciunas
ANL Patent Dept.
ANL Contract File
ANL Libraries (2)
TIS Files (6)

External:

DOE-TIC, for distribution per UC-11 (231)
Manager, Chicago Operations Office, DOE
Radiological and Environmental Research Division Review Committee:
- A. K. Blackadar, Pennsylvania State U.
- A. W. Castleman, Jr., Pennsylvania State U.
- R. E. Gordon, U. Notre Dame
- R. A. Hites, Indiana U
- D. Kleppner, Massachusetts Inst. Technology
- G. M. Matanoski, Johns Hopkins U.
- R. A. Reck, General Motors Research Lab.
- L. A. Sagan, Electric Power Research Inst.
- R. E. Wildung, Battelle Pacific Northwest Lab.

B. Ackerman, Illinois State Water Survey, Champaign
W. C. Ackermann, U. Illinois, Urbana
E. Adams, Massachusetts Inst. Technology
Air Pollution Control Association, Library, Pittsburgh
L. H. Allen, Jr., U. Florida
A. W. Andren, U. Wisconsin-Madison
R. A. Anthes, National Center for Atmospheric Research, Boulder
S. P. S. Arya, North Carolina State U.
D. Atlas, NASA Goddard Space Flight Center
Atmospheric Sciences Lab., White Sands Missile Range
E. J. Aubert, NOAA, Ann Arbor
S. I. Auerbach, Oak Ridge National Lab.
F. I. Badgley, U. Washington
R. H. Ball, Div. Environmental Issues, USDOE
D. S. Ballantine, Office of Health and Environmental Research, USDOE
M. L. Barad, Belmont, Mass.
S. Barr, Los Alamos National Lab.
A. M. Beeton, U. Michigan
S. Berman, State U. College at Oneonta, N. Y.
C. Bhumralker, SRI International, Menlo Park
E. Bierly, National Science Foundation

G. E. Birchfield, Northwestern U.
S. Booras, Illinois Inst. for Environmental Quality, Chicago
R. D. Bornstein, San Jose State U.
L. Botts, Northwestern U.
R. R. Braham, Jr., U. Chicago
S. D. Burks, Naval Environmental Prediction Research Facility, Monterey
J. A. Businger, National Center for Atmospheric Research, Boulder
S. H. Cadle, General Motors Research Labs.
California, U. of, Los Angeles, Chairman, Dept. of Meteorology
G. S. Campbell, Washington State U.
G. R. Carmichael, U. Iowa
H. Cember, Northwestern U.
J. E. Cermak, Colorado State U.
J. Chang, National Center for Atmospheric Research, Boulder
S. A. Changnon, Illinois State Water Survey, Champaign
R. J. Charlson, U. Washington
N. Chen, ATDL/NOAA, Oak Ridge
J. Ching, USEPA, Research Triangle Park
D. P. Chock, General Motors Corp., Warren, Mich.
T. L. Clark, USEPA, Research Triangle Park
W. E. Clements, Los Alamos National Lab.
J. Cocanougher, Miami U., Oxford, O.
Colorado State U., Library, Dept. of Atmospheric Sciences
Commonwealth Edison Co., Dept. of Environmental Planning, Chicago
Connecticut, U. of, Chairman, Dept. of Meteorology
Cornell U., Agricultural Experiment Station, Geneva
Cornell U., Librarian, Microclimatology Research Unit
R. B. Corotis, Johns Hopkins U.
S. Corrsin, Johns Hopkins U.
E. B. Cowling, North Carolina State U.
T. V. Crawford, Savannah River Lab.
C. T. Csanady, Woods Hole Oceanographic Inst.
R. C. Dahlman, Office of Basic Energy Sciences, USDOE
K. L. Davidson, U. S. Naval Postgraduate School
D. Davis, Georgia Inst. Technology
J. W. Deardorff, Oregon State U.
K. Demerjian, USEPA, Research Triangle Park
R. DePena, Pennsylvania State U.
M. Dickerson, Lawrence Livermore National Lab.
C. R. Dickson, NOAA, Idaho Falls
R. R. Draxler, Air Resources Labs., NOAA, Rockville
J. Droppo, Battelle Pacific Northwest Lab.
R. A. Duce, U. Rhode Island
Duke U., Chairman, Dept. of Environmental Science
J. L. Durham, USEPA, Research Triangle Park
A. Eddy, U. Oklahoma
D. N. Edgington, U. Wisconsin-Milwaukee
C. Elderkin, Battelle Pacific Northwest Lab.
W. P. Elliott, NOAA, Silver Spring
E. Eloranta, U. Wisconsin-Madison
E. S. Epstein, U. Michigan
G. H. Fichtl, NASA Marshall Space Flight Center
R. G. Fleagle, U. Washington
S. Friedlander, California Inst. of Technology

C. A. Friehe, U. California, Irbine
J. Friend, Drexel U.
J. Galloway, U. Virginia
A. A. Garrett, Savannah River Lab.
D. M. Gates, U. Michigan
D. F. Gatz, Illinois State Water Survey, Champaign
N. Gillani, Washington U.
J. C. Golden, Jr., Commonwealth Edison Co., Chicago
J. Goll, U. S. Minerals Management Service, Reston
W. Gray, Colorado State U.
T. J. Gross, Office of Basic Energy Sciences, USDOE
P. H. Gudiksen, Lawrence Livermore National Lab.
C. Hakkarinan, Electric Power Research Inst.
J. M. Hales, Battelle Pacific Northwest Lab.
F. F. Hall, NOAA, Boulder
S. R. Hanna, ERT, Inc., Concord, Mass.
Harvard U., Chairman, Dept. of Meteorology
D. A. Haugen, Wave Propagation Lab., NOAA, Boulder
Hawaii, U. of, Chairman, Dept. of Meteorology
J. L. Heffter, Air Resources Lab., NOAA, Rockville
B. B. Hicks, ATDL/NOAA, Oak Ridge
G. M. Hidy, Environmental Research & Technology Inc., Westlake Village, Calif.
G. Hilst, Electric Power Research Inst.
D. R. Hitchcock, Farmington, Conn.
W. Hooke, Wave Propagation Lab., NOAA, Boulder
T. W. Horst, Battelle Pacific Northwest Lab.
R. P. Hosker, Jr., ATDL/NOAA, Oak Ridge
A. H. Huber, USEPA, Research Triangle Park
R. B. Husar, Washington U.
IIT Research Institute, Document Library
Illinois Environmental Protection Agency, Manager, Div. of Air Pollution Control, Springfield
Illinois State Water Survey, Librarian, Champaign
Illinois, U. of, Chicago Circle Campus, Library
Iowa State U., Chairman, Dept. of Meteorology
J. Jansen, Southern Company Services, Inc., Birmingham
W. B. Johnson, SRI International, Menlo Park
J. C. Kaimal, Wave Propagation Lab., NOAA, Boulder
E. Klappenbach, USEPA, Chicago
H. Klieforth, Desert Research Inst., Reno
J. B. Knox, Lawrence Livermore National Lab.
C. W. Kreitzburg, Drexel U.
S. V. Krupa, U. Minnesota
M. Lazzaro, U. Chicago
H. H. Lettau, U. Wisconsin-Madison
D. K. Lilly, U. Oklahoma
M. K. Liu, Systems Applications, Inc., San Rafael
W. A. Lyons, Mesomet, Inc., Chicago
M. C. MacCracken, Lawrence Livermore National Lab.
W. M. Mach, Florida State U.
J. Mahlman, Princeton U.
L. Marht, Oregon State U.
E. Markee, Div. Reactor Licensing, USNRC
E. A. Martell, National Center for Atmospheric Research, Boulder

Maryland, U. of, Chairman, Dept. of Engineering
D. J. McNaughton, TRC Environmental Consultants, Inc., Salt Lake City
G. Mellor, Princeton U.
R. Meroney, Colorado State U.
Miami, U. of, Inst. of Atmospheric Science, Coral Gables
P. Michael, Brookhaven National Lab. (3)
Michigan, U. of, Great Lakes Research Div.
R. W. Miksad, U. Texas, Austin
E. Miller, Corvallis, Ore.
J. M. Miller, Air Resources Lab., NOAA, Rockville
T. A. Miskimen, American Electric Power Service Corp., New York
Missouri, U. of, Chairman, Dept. of Atmospheric Science, Columbia
Missouri, U. of, Chairman, Dept. of Meteorology, Rolla
K. Miyakado, Princeton U.
V. A. Mohnen, SUNY at Albany
E. L. Molle-Christensen, Massachusetts Inst. Technology
C. H. Mortimer, U. Wisconsin-Milwaukee
H. Moses, Office of Health and Environmental Research, USDOE
H. F. Mueller, NOAA, Las Vegas
P. K. Mueller, Electric Power Research Inst., Palo Alto
T. J. Murphy, DePaul U.
J. R. Murray, Murray & Trettle, Inc., Northfield, Ill.
C. J. Nappo, Jr., NOAA, Oak Ridge
NASA Goddard Space Flight Center, Librarian
NASA Langley Research Center, Technical Library
NASA Lewis Research Center, Librarian
National Center for Atmospheric Research, Library, Boulder
National Oceanic and Atmospheric Admin., Library, Silver Spring
National Weather Service, Headquarters, Silver Spring
W. D. Neff, Environmental Research Lab., Boulder
Nevada, U. of, Desert Research Inst.
R. E. Newell, Massachusetts Inst. Technology
L. Newman, Brookhaven National Lab.
New York, City U. of, Chairman, Dept. of Meteorology
G. Nichols, Jr., Manchester, Mass.
E. C. Nickerson, NOAA, Boulder
K. Noll, Illinois Inst. Technology
Northwestern U., Library, The Technical Institute
V. E. Noshkin, Lawrence Livermore National Lab.
Notre Dame, U. of, Library, Dept. of Meteorology
H. T. Odum, U. Florida
Y. Ogura, U. Illinois, Urbana
Oklahoma, U. of, Chairman, Dept. of Meteorology
R. E. Orville, SUNY at Albany
W. S. Osburn, Office of Health and Environmental Research, USDOE
H. G. Ostlund, U. Miami, Fla.
W. Ott, USEPA, Rockville
D. H. Pack, McLean, Va.
H. A. Panofsky, San Diego
D. Pashayan, USEPA, Washington
C. A. Paulson, Oregon State U.
W. Pennell, Battelle Pacific Northwest Lab.
L. K. Peters, U. Kentucky
J. H. Phillips, USEPA, Chicago

R. A. Pielke, Colorado State U.
G. W. Platzman, U. Chicago
D. Pogany, Illincis Div. of Energy, Springfield
J. M. Prospero, Rosensthiel School of Marine and Atmospheric Science, Miami
W. O. Pruitt, U. California, Davis
H. R. Pruppacher, U. California, Los Angeles
R. A. Ragotzkie, U. Wisconsin
D. Randerson, Air Resources Lab., NOAA, Las Vegas
S. Rao, ATDL/NOAA, Oak Ridge
G. S. Raynor, Brookhaven National Lab.
D. E. Reichle, Oak Ridge National Lab.
W. E. Reifsnyder, Yale School of Forestry and Environmental Studies
E. R. Reiter, Colorado State U.
Rhode Island, U. of, Chairman, Dept. of Environmental Science
J. Robbins, U. Michigan
E. Robinson, Washington State U.
G. D. Robinson, Center for the Environment and Man, Hartford, Conn.
N. J. Rosenberg, U. Nebraska
E. Ryznar, U. Michigan
P. Samson, U. Michigan
W. Saucier, North Carolina State U.
J. H. Saylor, NOAA, Great Lakes ERL, Ann Arbor
C. L. Schelske, U. Michigan
F. A. Schiermier, USEPA, Research Triangle Park
J. F. Schubert, Savannah River Lab.
S. Schwartz, Brookhaven National Lab.
R. Semonin, Illinois State Water Survey, Champaign
R. J. Serafin, National Center for Atmospheric Research, Boulder
S. SethuRaman, North Carolina State U.
J. Shinn, Lawrence Livermore National Lab.
H. Sievering, Governors State U., Park Forest South, Ill.
D. H. Slade, Office of Health and Environmental Research, USDOE
M. Smith, Smith-Singer Meteorologists, Inc., Massapequa, New York
W. H. Snyder, USEPA, Research Triangle Park
K. C. Spengler, American Meteorological Society, Boston
C. Spicer, Battelle Columbus Lab.
G. E. Start, NOAA, Idaho Falls
C. R. Stearns, U. Wisconsin-Madison
E. F. Stoermer, U. Michigan
R. H. Strange II, National Science Foundation
R. B. Stull, U. Wisconsin, Madison
J. Swinebroad, Office of Environment, Safety, and Health, USDOE
C. B. Tanner, U. Wisconsin-Madison
Tennessee, U. of, Chairman, Dept. of Meteorology
Texas A&M U., Librarian, Dept. of Oceanography and Meteorology
Texas, U. of, Atmospheric Science Group, Austin
D. W. Thomson, Pennsylvania State U.
K. H. Underwood, Zontech, Inc., Van Nuys
U. S. Dept. of Agriculture, Library, Washington
U. S. Dept. of the Interior, Bu. of Reclamation, Denver
U. S. Dept. of the Interior, Library, Washington
U. S. Dept. of Transportation, Librarian, Transportation Systems Center, Cambridge, Md.
U. S. Dept. of Transportation, Library, Washington

U. S. Environmental Protection Agency, Nat. Envtl. Res. Ctr., Cincinnati
U. S. Naval Postgraduate School, Chairman, Dept. of Meteorology
I. Van der Hoven, NOAA, Silver Spring
W. M. Vaughan, EMI, University City, Mo.
S. B. Verma, U. Nebraska-Lincoln
H. L. Volchok, Environmental Measurements Lab., USDOE, New York
J. A. Warburton, Desert Research Inst., Reno
J. A. Weinman, U. Wisconsin-Madison
L. L. Wendell, Battelle Pacific Northwest Lab.
R. E. Wildung, Battelle Pacific Northwest Lab.
M. H. Wilkening, New Mexico Inst. of Mining and Technology, Socorro
J. C. Willett, Naval Research Lab.
J. C. Wilson, U. Minnesota
W. E. Wilson, National Center for Air Pollution Control, USEPA, Research Triangle Park
J. W. Winchester, Florida State U.
Woods Hole Oceanographic Institution, Document Library
B. Wurful, U. California, Berkeley
J. C. Wyngaard, National Center for Atmospheric Research, Boulder
Wyoming, U. of, Dept. of Atmospheric Resources
Yale U., Chairman, Dept. of Geology and Geophysics
T. Yamada, Los Alamos National Lab.
R. Yamartino, Environmental Research and Technology, Inc., Concord, Mass.
J. Young, U. Wisconsin-Madison
H. Zar, USEPA, Chicago
K. Zar, U. Chicago
E. F. Bradley, C.S.I.R.O., Canberra City, Australia
C.S.I.R.O., Div. of Atmospheric Physics, Librarian, Mordialloc, Australia
C.S.I.R.O., Div. of Environmental Mechanics, Librarian, Canberra, Australia
Commonwealth Meteorology Research Centre, Librarian, Melbourne, Australia
J. R. Garratt, C.S.I.R.O., Mordialloc, Australia
G. D. Hess, Environmental Protection Authority of Victoria, East Melvourne, Australia
E. T. Linacre, Macquarie U., North Ryde, Australia
Melbourne, U. of, Librarian, RAAF Academy/Physics Dept., Australia
J. R. Philip, C.S.I.R.O., Canberra, Australia
P. Schwerdtfeger, Flinders U. of South Australia, Bedford Park, Australia
N. A. Shaw, Footscray Inst. Technology, Footscray, Australia
S. Turner, Australian National University, Sutherland
Canada Centre for Inland Waters, Librarian, Burlington
A. G. Davenport, U. Western Ontario, London, Canada
F. Elder, Canada Centre for Inland Waters, Burlington
J. Gannon, International Joint Commission, Windsor, Canada
K. D. Hage, U. Alberta, Edmonton, Canada
D. N. Kirshak, Ontario Hydro, Toronto, Canada
H. C. Martin, Atmospheric Environment Service, Downsview, Canada
McGill U., Chairman, Dept. of Meteorology, Montreal, Canada
W. J. Moroz, Ontario Hydro, Toronto, Canada
R. E. Munn, U. Toronto, Canada
T. R. Oke, U. British Columbia, Vancouver, Canada
L. Shenfeld, Ministry of the Environment, Toronto, Canada
P. A. Taylor, Atmospheric Environment Service, Downsview, Canada
G. W. Thurtell, Guelph, Canada
Toronto, U. of, Library, Serials Dept., Canada

T. Turner, Atmospheric Environment Service, Downsview, Canada
E. Voldner, Atmospheric Environment Service, Downsview, Canada
R. A. Vollenweider, Canada Centre for Inland Waters, Burlington
D. M. Whelpdale, Atmospheric Environment Service, Downsview, Canada
C-Y. Tseng, Inst. of Physics, Nankang, Taiwan, China
M-Y. Chou, Academia Sinica, Beijing, People's Republic of China
X-F. Zhang, Academia Sinica, Beijing, People's Republic of China
N. E. Busch, Danish AEC, Risø
L. Kristenson, Risø National Lab., Roskilde, Denmark
L. Prahm, Risø National Lab., Roskilde, Denmark
A. C. Chamberlain, UKAEA, Harwell, England
J. Garland, AERE, Harwell, England
Inst. of Oceanographic Sciences, Librarian, Wormley, England
P. Liss, U. East Anglia, Norwich, England
Meteorological Office Library, Bracknell, England
F. B. Smith, Meteorological Office, Bracknell, England
P. A. Taylor, U. Southampton, England
L. Hasse, Institut für Meerskunde, Kiel, Germany
D. Lege, U. Hannover, Germany
Meteorologisches Inst. der Universitat Hamburg, Librarian, Germany
K. O. Munnich, Physikalische Inst. der Universitat Heidelberg, Germany
R. Roth, Technischen Universitat Hannover, Germany
Y. Neumann, U. Jerusalem, Israel
O. Vittori, Laboratorio Microfisica dell' Atmosfera, Bologna, Italy
E. Inoue, National Inst. of Agricultural Sciences, Tokyo, Japan
K. Kitabayashi, National Res. Inst. for Pollution and Resources, Tokyo, Japan
Y. Ogawa, National Inst. for Environmental Sciences, Tokyo, Japan
K. Sahashi, Okayama U., Japan
H. Tennekes, Royal Netherlands Meteorological Inst., Debilt
R. M. van Aalst, TNO, Delft, The Netherlands
A. Eliassen, Norwegian Meteorological Inst., Oslo
D. T. Gjessing, Norwegian Defense Research Establishment, Kjeller
L. Granat, U. Stockholm, Sweden
Swedish Meteorological and Hydrological Inst., Norrköping
Academy of Sciences of the USSR, Librarian, Inst. of Atmospheric Physics, Moscow